Metrological triangulation rules in ratio measurements of high standard resistance bridges

Iulian Mihai

Metrological triangulation rules in ratio measurements of high standard resistance bridges

R.T. 19/2022 May 2022

I.N.RI.M. TECHNICAL REPORT

Abstract

At the National Institute of Metrological Research (INRiM) a first evaluation for systematic errors of a commercial dual source high resistance bridge has been made using restrictive metrological triangulation rules. This technical report exploits the use of the Allan variance and the spectral power density to achieve optimum performances and its limits in case of the high resistance measurement modified Wheatstone bridge of commercial type. The study was performed observing the ratios measurements of the bridge for the standard resistors in the range from 10 TΩ to 1 PΩ.

Keywords: High resistance measurements, metrological triangulation rules, measurement uncertainty, compatibility test, measurement noise.

Sommario

Presso l'Istituto Nazionale di Ricerca Metrologica (INRiM) è stata effettuata una prima valutazione degli errori sistematici per un ponte commerciale ad alta resistenza a doppia sorgente utilizzando regole di triangolazione metrologica restrittive. Questa relazione tecnica sfrutta l'uso della varianza di Allan e della densità di potenza spettrale per ottenere i limiti di queste regole nel caso del ponte di Wheatstone modificato di tipo commerciale. Lo studio è stato condotto osservando le misure di rapporto di resistenze campione nel campo da 10 TΩ a 1 PΩ.

Keywords: Misure di resistori campioni di alto valore, regole di triangolazione metrologica, incertezza di misura, test di compatibilità, misure affette da rumore.

Duane Brown / Measurements International, Canada

Senior Member IEEE
Measurements International

I have been asked to write an opinion on a report titled

Metrological triangulation rules in ratio measurements
of high standard resistance bridges
By Iulian Mihai, I.N.RI.M. TECHNICAL REPORT, May 2022

The report is based on high value resistance measurements from 10 TΩ to 100 TΩ using a Measurements International Model 6600A Dual Source Resistance Bridge. The aim of this project is the identification of systematic errors, by means of the metrological triangulation rules, to be used successively to carry out calibration services in terms of the ISO 17025 in achieving the best minimum value of the mean and standard deviation for each ratio. In my opinion the paper covers the general guidelines for technical papers covering Abstract, Introduction, Hypothesis, Data sampling including Results and Discussions, Conclusion, and References.

In this report the Metrological triangulation rules in ratio measurements are where accurate measurements of high value resistors using a commercial off the shelf resistance bridge can be determined and verified. The paper is well written featuring many diagrams and flow charts, and one can learn a lot about understanding high resistance measurements using triangulation rules to help understand the measurement noises and instabilities that have been detected at 100 TΩ 1 PΩ.

The technical report also exploits the use of Spectral Power density and the Allan variances to analyze the performance of the high resistance measurement bridge to determine the number of the detector readings for each measurement. This was intriguing and something new to me. Once determined this can be accomplished at different ratios and voltages and was quite exciting as the number of measurements could be reduced considerably.

Future aims of the work will be the implementation of a triangular ratio test consisting of a comparison between a 10 TΩ, 100 TΩ and a 1 PΩ resistor to verify the metrological triangulation rules at 250V, 500V, 750 V and 950 V. Not many NMI's are working in improving measurements in this range.

All in all a very good paper full of knowledge, data and ideas.

Sommario

1. INTRODUCTION

This technical report explores metrological triangulation rules in ratio measurements using also the technique of Allan variance and the power spectral density, familiar in the time and frequency metrology, in order to improve the performance in high resistance measurement systems and to solve the systematic errors or functioning errors of the commercial bridge 6600A. These tools have been used in the past by the author of this work also to optimize a bridge based on a cryogenic current comparator. The data correlation due to 1/f noise of the current measured by the detector and the unbalance parameter used by the bridges has a great impact on measurement distribution and standard deviation. In particular, a series of non-correlated data, the distribution is characterized by the standard deviation of the mean. For correlated data, this statement is no longer valid. Measuring for any longer than the optimum unbalance steps for the measurement bridge is counterproductive, as the random drift will start to dominate. In addition, failure to correctly treat correlations can produce significant errors in any Type A uncertainty. One application of such evaluation concerns the measurement of standards resistors in the TΩ range with a modified Wheatstone bridge. The predominantly aim of this work is the identification of systematic errors, by means of the metrological triangulation rules, in order to be used successively to carry out calibration services in terms of the ISO 17025.

The author wishes to express his profound thanks to Mr. **Duane Brown** from Measurements International, Canada for his help with the 6600A bridge's operation and many useful suggestions and to Mr. **Richard Timmons**, President of Guildline Instruments, Canada for helping me with the standard resistor of 100 TΩ used also during the comparison EURAMET.EM-S32: "Comparison of resistance standards at 1 TΩ and 100 TΩ" and taking the time to read this technical report. Special thanks to Mr. **Paul Crowhrust** from Evolution Measurement, United Kingdom and to Mr. **Giuseppe Ronciglia**, Mr. **Jacopo Grazzini** from **EvoMisure,** Italy for lending me the standard resistor from Guildline.

20 May 2022

2. HIGH RESISTANCE MEASUREMENT BY MEANS OF THE MODIFIED WHEATSTONE BRIDGE

In the modified Wheatstone bridge a measurement consists of balancing of the bridge, followed by a waiting time for the stabilization and data acquisition from the current detector. At fixed voltage V_x, the voltage V_s is varied until the current reading of the detector I_D corresponds to the reading at zero voltage ($V_x = V_s = 0$) measurements over the resistors under measurement R_x and standard resistor R_s. The measurement is repeated at reversed polarity of two DC voltage calibrators. The schematic principle of the bridge is shown in Figure 1.

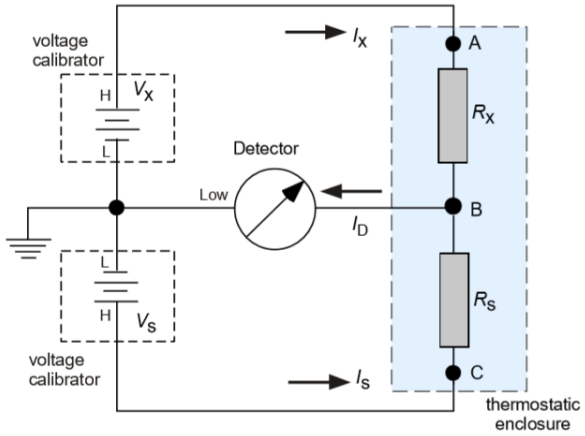

Figure 1. The principle of a Wheatstone modified bridge.

The low circuit impedance of the detector means that the current flowing in each resistor is determined by the voltage source effectively connected across it. The voltage ratio is set up such that these currents are in opposition and the detector measures the difference between these two currents. The mean detector reading is used to calculate a corrected final balance reading. The DC current I_D measured by the detector is given by the sum of the currents flowing in the arms of the bridge I_s and I_x :

$$I_D = I_s + I_x = \frac{V_s}{R_s} + \frac{V_x}{R_x} \tag{1}$$

The resistance ratio r is calculated as the ratio between the resistors under measurement R_x and standard resistor R_s at the condition $I_D \cong 0$:

$$r = \frac{R_x}{R_s} = \left| -\frac{V_x}{V_s} \right| \tag{2}$$

The value of the measurand R_x is obtained using the equation (2). In practice, the value of I_D measured by a current detector is used to calculate the equivalent value of voltage V_s.

For the measurements with a high resistance value, it is important to define the measurand whose purpose is to define a closed geometric surface and a set of electrical boundary conditions, in an attempt to exclude any effect due to connections, cables and the electromagnetic properties of the environment, so that changes in these have no effect on the measurements. In standard resistors, a shield often identifies the geometric surface, and connectors mounted on the housing define the type of connection. The high value resistor is a resistor with three terminals: Source, Output (or Hi and Lo) and one terminal connected to the shield, as shown in Figure 2 a) and b). In Figure. 2. a) the resistance is the results of a network of dividing networks (R_i, R_0) and the leakage resistor R_d. Considering that the Output terminal and the shield are at the same potential, the resistance of the measurand R_x between the source terminal and the output terminal is given by the combination of the three resistors. In Figure 2. b) the resistor has two shields (inside and outside). The internal shield, part in glass and part in metal, is loaded with a dry gas (argon) and contains the resistive element. The two metal ends of the inner shield are isolated from each other and connected to the N-type connectors isolated from the outer shield. An additional terminal is used for connection to the ground potential.

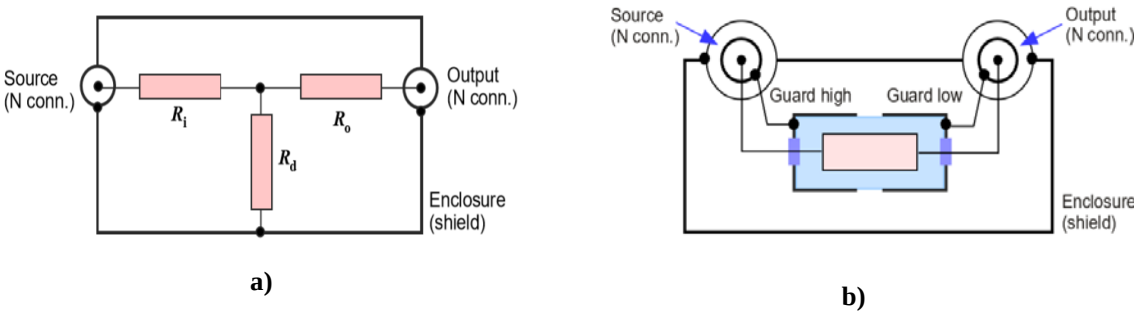

Figure 2. Representation of the high value resistors. The shield delimits the electrical resistance inside and outside the ports Source and Output. a) network resistors b) unique resistive element.

Repeating the measurements at reversed polarity of two DC voltage calibrators, the measurement bridge eliminates the calibrator offset and eliminates the effect of the thermal forces (emfs). By doing this, possible offsets can be removed from the final result.

The mean value of the resistance ratio $\bar{r}$ at the end of the measurement session is given by:

$$\bar{r} = \frac{1}{N_r}\sum_{i=1}^{N} r_i \qquad (3)$$

Where N_r is the number of the repetitions. So, the value of the measurand is: $R_x = \bar{r} \cdot R_s$
When the mean value is calculated from a set of individual values, which are randomly distributed, then the mean value will also be a random quantity. As for any random quantity, it is also possible to calculate standard deviation for the mean (sdvm) u_r , dividing the standard deviation by square root of the number of repeated measurements N_r.

AUTOMATED DUAL SOURCE HIGH RESISTANCE RATIO BRIDGE

The National Institute of Metrology (INRiM) uses as a modified Wheatstone bridge the commercial measurement bridge, MI 6600A Automated Dual Source High Resistance Ratio Bridge. This measurement bridge consists of two model 1000C DC voltage sources that are

programmable to 1000V, an Input Signal Interface model MI 8100, and an electrometer / detector of type Keithley 6514 [1]. The detector measures the current difference flowing through the two resistors placed on the two active arms of the measurement bridge. MI 6600A bridge [2] is located inside a shield room in a laboratory and it is connected independently to the ground potential. The MI 6600A and accessories are controlled through the IEEE488 Interface Bus using the supplied 6600A Software of version 2.2.0 and by an external computer running the program task from the outside the shielded room. The shield room ambient conditions are (23.0 ± 1.0) °C and (45 ± 10) % RH. The resistors under comparison (R_x and R_s), are connected to the front terminal R1, respectively, R2 of the unit 8100 Input Signal Interface by means of the RG58 coaxial cables to the voltage supply S1, respectively, S2 [3] as shown in Figure 3. The resistors under comparison are kept during measurements at a more stable condition in a thermostatic chamber at (23.0 ± 0.1) °C controlled by a Peltier regulating from outside thermostatic chamber. The relative humidity is less than 40 % RH obtained by means of hygroscopic salts, to reduce the interference and noise, that is disposed at the base of the chamber between its bottom and a flat that sustain the resistors [4, 5, 6].

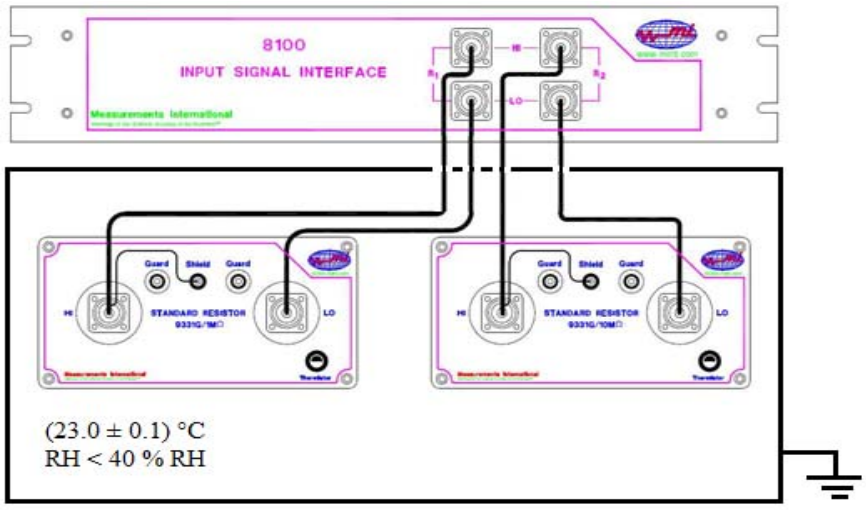

Figure 3. Connection to the front panel of the Input Signal Interface. The bold line indicates the thermostatic chamber shielded, connected to the ground potential.

The two sources are calibrated using a high precision digital voltmeter HP3458, calibrated within 24 hours by the national calibration laboratory. The DVM is connected to the computer

via the rear panel connectors and the software version 2.2.0. In addition, the current detector Keithley 6514 is also calibrated by national laboratory and the software of the bridge adjusts for the errors presented in the calibration certificate.

MEASUREMENT COMPARISONS WITH THE BRIDGE MODEL MI 6600A

In this work the measurements are performed by means of two comparisons between one resistors of 10 TΩ as standard resistor R_s and two resistors of 100 TΩ as measurand R_x, and another two comparisons between the two resistors of 100 TΩ at the test DC voltages of 250 V, 500 V, 750 V and 1000 V. The Figure 4 shows in a schematic way these comparisons. The resistors used in this work are shown in the Table 1 and the comparisons are shown in Table 2.

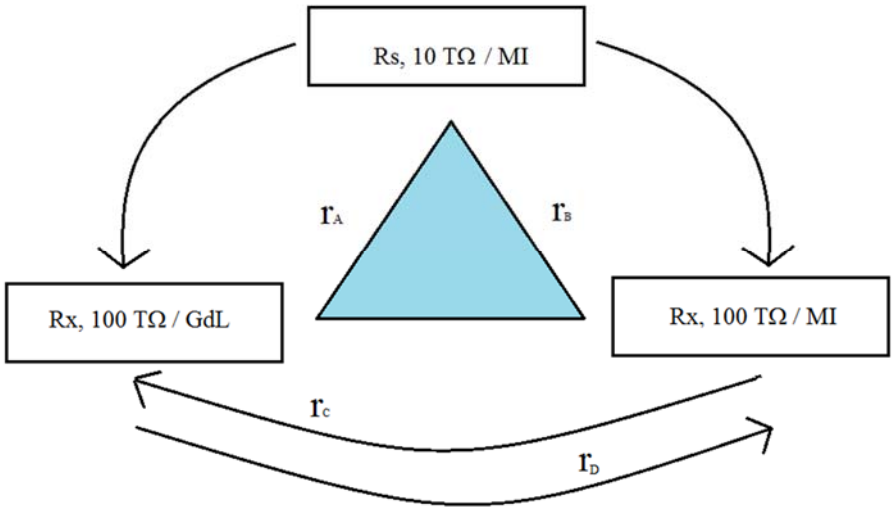

Figure 4. The ratio measurement comparisons between high value resistors and their resistance.

Table 1. The resistors used in this comparison and their typologies.

Resistors R_s, R_x	**Serial number**	**Model**
R_s, 10 TΩ / MI	1101167	MI 9331G/10TΩ
R_x, 100 TΩ / MI	1101170	MI 9331G/100TΩ
R_x, 100 TΩ(1) / GdL	69640	Guildline 9337-100T

Note (1). This costumer resistor is the property of Guildline and it was part of the comparison EURAMET.EM-S32: "Comparison of resistance standards at 1 TΩ and 100 TΩ".

Table 2. The resistors used in this comparison and their ratio.

Comparison		Ratio	Mean resistance ratio, $\bar{r}$	Standard deviation of the mean u_r , (ppm)
A.	R_s, 10 TΩ / MI : R_x, 100 TΩ / GdL	1 : 10	$\overline{r_A}$	u_{rA}
B.	R_s, 10 TΩ / MI : R_x, 100 TΩ / MI	1 : 10	$\overline{r_B}$	u_{rB}
C.	R_s, 100 TΩ / MI : R_x, 100 TΩ / GdL	1 : 1	$\overline{r_C}$	u_{rC}
D.	R_s, 100 TΩ / GdL : R_x, 100 TΩ / MI	1 : 1	$\overline{r_D}$	u_{rD}

Using the triangulation rules, the value of the ratio measured in the first comparison $\overline{r_A}$, should be as close as possible to product of the second and third comparisons, $\overline{r_B}$ and, respectively, $\overline{r_C}$, given by:

$$\overline{r_A} \cong \overline{r_B} \cdot \overline{r_C} \quad \text{or, as expressed in ppm,} \quad \left(1 - \frac{\overline{r_A}}{\overline{r_B} \cdot \overline{r_C}}\right) \cdot 10^6 \cong 0 \tag{4a}$$

On the other hand, the value of the ratio measured in the first comparison $\overline{r_A}$ and the fourth comparison $\overline{r_D}$, should be as close as possible to the second comparisons $\overline{r_B}$, given by:

$$\overline{r_B} \cong \overline{r_A} \cdot \overline{r_D} \quad \text{or, as expressed in ppm,} \quad \left(1 - \frac{\overline{r_A} \cdot \overline{r_D}}{\overline{r_B}}\right) \cdot 10^6 \cong 0 \tag{4b}$$

To achieve this rule, it can be accepted the metrological triangulation condition:

$$\left(1 - \frac{\overline{r_A}}{\overline{r_B} \cdot \overline{r_C}}\right) \cdot 10^6 < \sqrt[2]{u_{rA}^2 + u_{rB}^2 + u_{rc}^2} \tag{5a}$$

$$\left(1 - \frac{\overline{r_A} \cdot \overline{r_D}}{\overline{r_B}}\right) \cdot 10^6 < \sqrt[2]{u_{rA}^2 + u_{rB}^2 + u_{rD}^2} \tag{5b}$$

To perform these comparisons, the MI 6600A bridge can be used either in quick mode or Single Measurement after selecting the desired setup for the resistors under comparison or Multiple Measurements after selecting Bridge Mode. To create programs, resistors have to

have been entered in the Resistor ID Listings through the Create/List Resistor ID Menu, and a Measurement, Task and Program have been created using the 'Programs' tab (under the 'Program Selection' menu), available to the Bridge Mode/ Multiple Measurements Screen. When it is necessary for example to evaluate the voltage dependence of Rx the Multiple Measurements mode is needed. It consists of programmed multiple repetitions of sessions of Single Measurement mode for the same ratio, each under different conditions as voltages, settle times, no. of measurements. A useful application of the Multiple Measurements mode is the Auto-Update function that automatically updates the R_x value at each measurement session. Increasing the settle time at each session, for example starting from the R_x time constant τ or its half in the first session and to its multiples in the following sessions, updating the R_x value allows the unbalance window to be reduced at each session minimizing the residual current at the detector approaching at best the ideal bridge balance. Taking advantage of these iterative steps, investigations on the improving of the bridge precision were made. This work is performed using Multiple Measurement and use the resistors R_s and R_x from Table 1 and the comparison shown in the Table 2. In addition, the bridge can be programed for different comparisons using fixed parameters, as test voltage, and variable settle time, as shown in Table 3, in agreement with other experimental report. The time constant obtained for the second comparison, between R_s, 10 TΩ / MI : R_x, 100 TΩ / MI is used also for the other two comparisons R_s, 100 TΩ / MI : R_x, 100 TΩ /GdL because the resistors with unique resistive element have a time constant longer in comparison with the network resistors.

Table 3. Settle time t_a for the ratios from Table 2.

Ratio	Time constant, (s) $t_a = \tau$
1: 10; 1 : 1	600

Before any comparison an initial test predicts that, if after the first check of the unbalance window, the equilibrium is not obtained, the program repeats the measurement by doubling the initial value. This is repeated three times after which, if there is still a balancing failure, the program stops and goes to Exit. If so, the program measures with positive polarity of V_x and subsequently, with reversed polarity. During Voltage Polarity Reversal, the MI 6600A

takes the average of two readings, one of each polarity, to calculate the resistor and the ratio values $\overline{r_A}$, $\overline{r_B}$ and, respectively, $\overline{r_C}$. The value of the device under test, the measurand, is always taken as the value extrapolated to complete stabilization, with no residual RC components in the measured signal. This work uses two measurement flowchart methods as reported in Figure 5 and 6 and described in the next paragraphs.

FLUX DIAGRAM WITH A CONSTANT SETTLE TIME.
MEASUREMENT PROGRAM PROG**1**

This flux diagram performs fifty ratio measurements between resistors at a constant settle time, as reported in the Table 4 for the entire period of the comparison. This task is repeated for the test voltages of 250 V, 500 V, 750 V and 1000 V. The results of the first method are three ratios $\overline{r_{A0}}$, $\overline{r_{B0}}$,$\overline{r_{C0}}$ and $\overline{r_{D0}}$.

Table 4. Measurement program at a fixed settle time and four test voltages.

Task	***Ratios***	**Settle time, (s)**	**Unbalance, (ppm)**	**Test, (V)**
1	$\overline{r_{A0/250}}$, $\overline{r_{B0/250}}$, $\overline{r_{C0/250}}$, $\overline{r_{D0/250}}$	3τ ≅ 1800 s	40001	250
2	$\overline{r_{A0/500}}$, $\overline{r_{B0/500}}$, $\overline{r_{C0/500}}$, $\overline{r_{D0/500}}$	3τ ≅ 1800 s	20001	500
3	$\overline{r_{A0/750}}$, $\overline{r_{B0/750}}$, $\overline{r_{C0/750}}$, $\overline{r_{D0/750}}$	3τ ≅ 1800 s	13334	750
4	$\overline{r_{A0/1000}}$, $\overline{r_{B0/1000}}$, $\overline{r_{C0/1000}}$, $\overline{r_{D0/1000}}$	3τ ≅ 1800 s	10001	1000

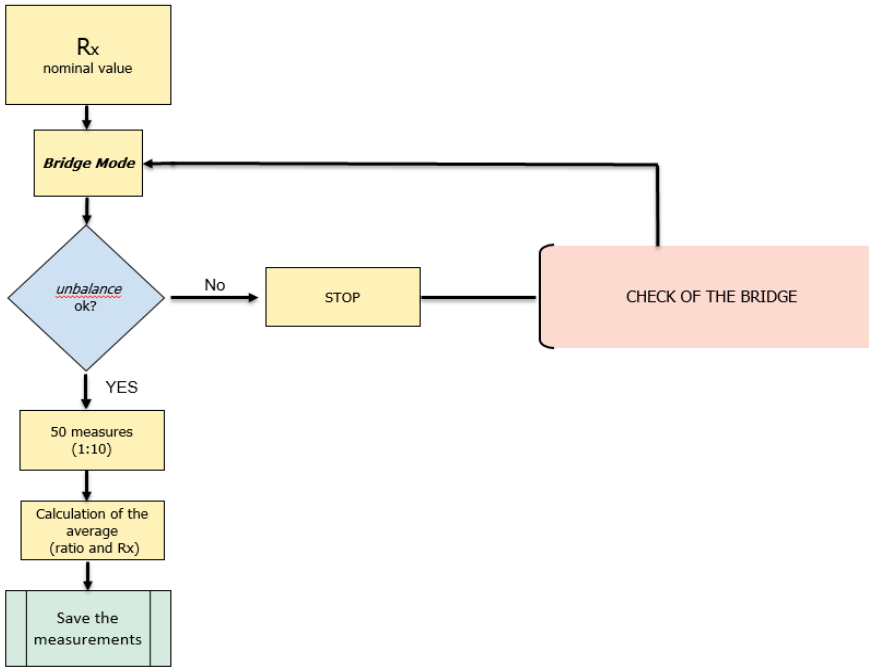

Figure 5. Flux diagram with a constant settle time (ratios 1:10 and 1:1).

The voltage across R_s remains constant during the whole runs at the equivalent test voltages of 25 V, 50 V, 75 V and 100 V from the task 1 to task 4. The equations 5a) and, respectively, 5b) can be written for each test voltage of 250 V, 500 V, 750V and 1000 V:

Task	**Equations 5a)** (ppm)	**Equations 5b)** (ppm)
1, 2, 3, 4	$\left(1-\frac{\overline{r_{A0}}}{\overline{r_{B0}}\cdot\overline{r_{C0}}}\right)\cdot 10^6 < \sqrt[2]{u_{rA0}^2+u_{rB0}^2+u_{rc0}^2}$	$\left(1-\frac{\overline{r_{A0}}\cdot\overline{r_{D0}}}{\overline{r_{B0}}}\right)\cdot 10^6 < \sqrt[2]{u_{rA0}^2+u_{rB0}^2+u_{rD0}^2}$

FLUX DIAGRAM WITH A VARIABLE SETTLE TIME.
MEASUREMENT PROGRAM PROG**2**

In the second method, the situation from the 1st flux diagram is repeated but at different settle time in 4 steps with fixed test voltage and a reduced number of measurements, from fifty to twenty. With the new obtained value of R_x with twenty measurements from the 2nd run, by means of the Auto Update function, and using it as R_x in the 3rd run, and so on, the last 3 programs are already within the unbalance window. The results of this comparison with this second method are three ratios $\overline{r_{A4}}$, $\overline{r_{B4}}$, $\overline{r_{C4}}$ and $\overline{r_{D4}}$.

Table 5. Measurement program at a variable settle times and a fixed test voltage of 1000V.

Task	*ratios*	Settle time, (s)	Unbalance(1), (ppm)	Test, (V)
1	$\overline{r_{A1/1000}}$, $\overline{r_{B1/1000}}$, $\overline{r_{C1/1000}}$, $\overline{r_{D1/1000}}$	1/2τ ≅ 300 s	10001	1000
2	$\overline{r_{A2/1000}}$, $\overline{r_{B2/1000}}$, $\overline{r_{C2/1000}}$, $\overline{r_{D2/1000}}$	1τ ≅ 600 s	-	1000
3	$\overline{r_{A3/1000}}$, $\overline{r_{B3/1000}}$, $\overline{r_{C3/1000}}$, $\overline{r_{D3/1000}}$	2τ ≅ 1200 s	-	1000
4	$\overline{r_{A4/1000}}$, $\overline{r_{B4/1000}}$, $\overline{r_{C4/1000}}$, $\overline{r_{D4/1000}}$	3τ ≅ 1800 s	-	1000

Note: During the iterations from task 1 to task 4 the value of the unbalance becomes less than the initial value.

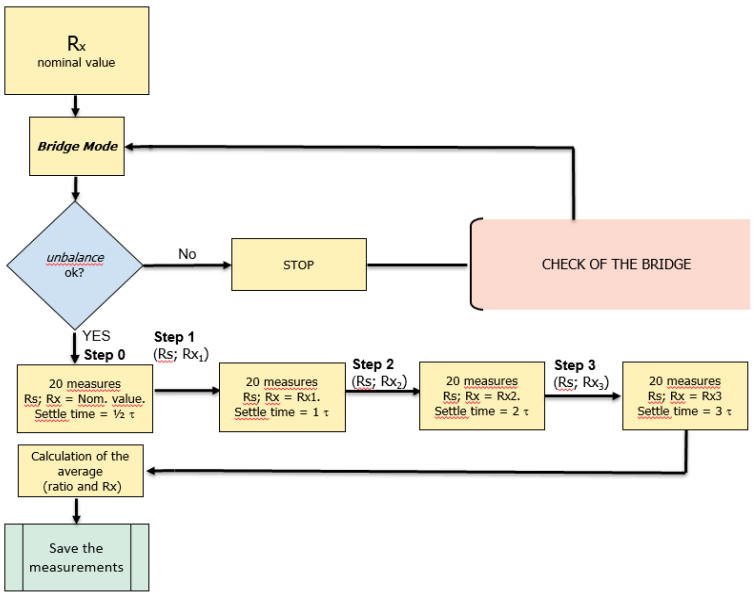

Figure 6. Flux diagram with a variable settle time (ratios 1:10 , 1:1).

The voltage across R_x does not remain constant (at the test voltages of 250 V, 500 V, 750 V and 1000 V) during the four steps as it changes according with the new unbalance parameter. At the end of each iteration, the value of each ratio is also updated. The equations 5a) and, respectively, 5b) can be written at the test voltages of 250 V, 500 V, 750 V and 1000 V:

Task	**Equations 5a),** (ppm)	**Equations 5b),** (ppm)
1	$\left(1-\frac{\overline{r_{A1}}}{\overline{r_{B1}}\cdot\overline{r_{C1}}}\right)\cdot 10^6 < \sqrt[2]{u_{rA1}^2+u_{rB1}^2+u_{rc1}^2}$	$\left(1-\frac{\overline{r_{A1}}\cdot\overline{r_{D1}}}{\overline{r_{B1}}}\right)\cdot 10^6 < \sqrt[2]{u_{rA1}^2+u_{rB1}^2+u_{rD1}^2}$
2	$\left(1-\frac{\overline{r_{A2}}}{\overline{r_{B2}}\cdot\overline{r_{C2}}}\right)\cdot 10^6 < \sqrt[2]{u_{rA2}^2+u_{rB2}^2+u_{rc2}^2}$	$\left(1-\frac{\overline{r_{A2}}\cdot\overline{r_{D2}}}{\overline{r_{B2}}}\right)\cdot 10^6 < \sqrt[2]{u_{rA2}^2+u_{rB2}^2+u_{rD2}^2}$
3	$\left(1-\frac{\overline{r_{A3}}}{\overline{r_{B3}}\cdot\overline{r_{C3}}}\right)\cdot 10^6 < \sqrt[2]{u_{rA3}^2+u_{rB3}^2+u_{rc3}^2}$	$\left(1-\frac{\overline{r_{A3}}\cdot\overline{r_{D3}}}{\overline{r_{B3}}}\right)\cdot 10^6 < \sqrt[2]{u_{rA3}^2+u_{rB3}^2+u_{rD3}^2}$
4	$\left(1-\frac{\overline{r_{A4}}}{\overline{r_{B4}}\cdot\overline{r_{C4}}}\right)\cdot 10^6 < \sqrt[2]{u_{rA4}^2+u_{rB4}^2+u_{rc4}^2}$	$\left(1-\frac{\overline{r_{A4}}\cdot\overline{r_{D4}}}{\overline{r_{B4}}}\right)\cdot 10^6 < \sqrt[2]{u_{rA4}^2+u_{rB4}^2+u_{rD4}^2}$

The measurement time used for the measurements with the constant settle time is equal with the measurement time used for the measurements with the variable settle time. The measurement with the constant settle time at each test voltages needs about 29 hours and in case of the ratio 1:1 the total voltages is 1000 V on each calibrator, reaching a difference potential of about 2000V.

EVALUATION OF THE INTRINSIC NOISE OF THE DC SOURCES

The technical report exploits the use the spectral power density and the Allan variances to analyze the performance of the high resistance measurement bridge of commercial type MI 6600A to determine the number of the detector readings for each measurand ratio and for both polarities, obtained using the equation (2). This technique was applied also to other measurement systems focusing on the characterization or optimization of the measurement and the improvement of the uncertainty. [7, 8, 9, 10, 11]. In this case, this technique was performed by observing the current measurements of the bridge detector as a function of its

integration time. As observed the noise is an undesired parameter in the sampled signals. It limits the attainable standard deviation of the estimated parameters, retrieved from sampled data. It is therefore important to know the noise limitations used for measuring sampled signal parameters at the lowest attainable uncertainties, which would be fundamentally limited by noise in the sampled signal. The data correlation due to 1/f noise has a great impact on measurement distribution and standard deviation. For a series of non-correlated data, the distribution is characterized by the standard deviation of the mean. For correlated data, this statement is no longer valid.

THE SPECTRAL POWER DENSITY AND THE ALLAN VARIANCE

One application of such evaluation concerns the measurement of standards resistors from Table 1. The aim of this work is the identification of the white noise regime, in order to be used successively to carry out electrometer readings for the high value resistances of 10 TΩ and 100 TΩ in direct current with the modified Wheatstone bridge of a commercial type [5].

For a continues function *y(t),* assumed to be periodical in the time interval t_T, the Fourier Transform (FFT) $F_y(f, t_T)$ is given by the equation:

$$F_y(f, t_T) = \int_0^{t_T} y(t) e^{-j(2\pi f t)} dt \tag{6}$$

The FFT returns a two-sided spectrum in complex form (real and imaginary parts), which must be scaled and converted to polar form to obtain magnitude and phase. The frequency axis is identical to that of the two-sided power spectrum. The amplitude of the FFT is related to the number of points in the time-domain signal. The two-sided amplitude spectrum actually shows half the peak amplitude at the positive and negative frequencies.

The power spectral density *PSD*(*f*) is computed from the FFT function and is given by the equation:

$$PSD_y(f) = \lim_{t_T \to \infty} \frac{2}{t_T} \left| F_y(f, t_T) \right|^2 \tag{7}$$

The power spectral density $PSD_y(f)$ of a time series $\bar{y}_l(\tau_0)$ can be modelled according to the following power law [10, 11]:

$$PSD(f) = \sum_{i=-2}^{2} \gamma_i f^i \tag{8}$$

Where the intensity coefficient γ_i and the index *i* depend on the type of noise.

The Allan variance $\sigma_y^2(\tau)$ and the power spectral density $PSD_y(f)$ corresponding to the three types of low frequency noise are reported in Table 6.

Table 6. Three types of low frequency noise.

Type	$\boldsymbol{PSD_y(f)}$	$\boldsymbol{\sigma_y^2(\tau)}$
white noise	γ_0	$\gamma_0/(2\tau)$
1/f noise	$\gamma_{-1} f^{-1}$	$2\gamma_{-1} ln(2)$
Random wall noise	$\gamma_{-2} f^{-2}$	$\frac{2}{3}\pi^2 \gamma_{-2} \tau$

In this table it can be observed that, in the case of white noise, the Allan standard deviation is proportional to $\tau^{-1/2}$. For random walk noise the Allan deviation increases with the square root of the integration time. The power spectral density is constant for white noise and is inversely proportional to the frequency for 1/f noise. The most common method for power law noise identification is simply to observe the slope of a log-log plot of the Allan deviation versus averaging time, either manually or by fitting a line to it.

EXPERIMENTAL SETUP

For the evaluation of the intrinsic noise of the DC current measured by the detector during the comparisons, an analysis of the direct Fourier transform of the signal obtained from the signal supplied by the detector to its 2 V output, an oscilloscope from Tektronix , Model TDS 3032 is used, equipped with the FFT module of type TDS 3FFT. Its battery supplies the oscilloscope power, and it is connected at the output of the detector by means of 50 Ω cables, outside the shielded room. The input current I_D is converted to a voltage and supplied to the 2V output signal of the detector. It provides a scaled ± 2 V that is inverting in the current mode measurement, as shown in Figure 7.

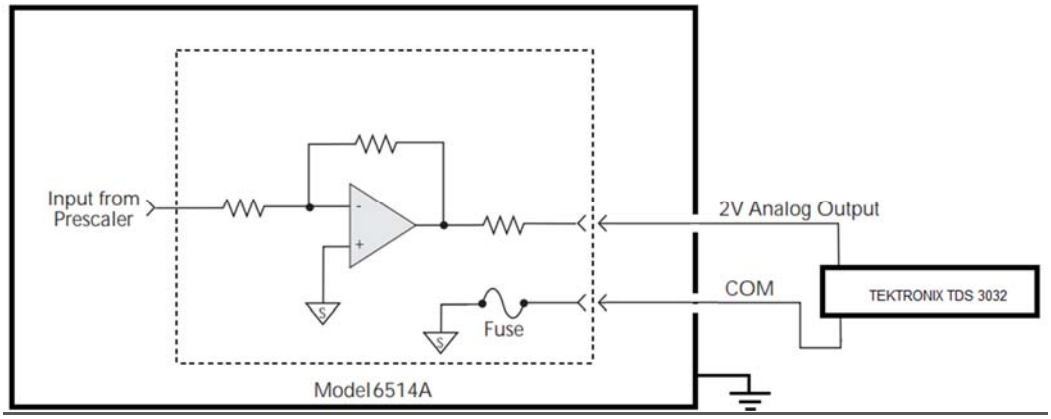

Figure 7. Output circuit to 2 V connection at the voltage input of the oscilloscope Tektronix, model TDS 3032. The bold line indicates the shielded room of the laboratory, connected to the ground potential.

The Fourier Transform is obtained with the module TDS 3032 of the scope with the setup parameters on Channel 1: 50 mV/div; 100 Sample/s, Band 20 MHz and the Hanning's window.

For the noise evaluation from the equation (8), it uses the free software program Stable32 and Microsoft Windows operation system for editing, simulation, analysis of the data and plotting. It is used by leading government and commercial metrology laboratories around the world, can be obtained free of charge from:

https://ieee-uffc.org/technical-committees/frequency-control/educational-resources/frequency-control-software

This program software is in compliant with IEEE Std 1139-2008 – IEEE Standard Definitions of Physical Quantities for Fundamental Frequency and Time Metrology – Random Instabilities. Stable32 file operations include opening data files, combining data, and storing all or a portion of the data. Data is stored in ASCII format, with gaps indicated by a value of zero, and may be inputted from any source that generates up to 8 columns of such comma or space-delimited data, with or without timetags. All storage and calculations of the equation are performed with double precision for a virtually unlimited number of data points. Plotting and printing can be done for all or a portion of the data, with drift fits and automatic or user-defined scales and titles. Analysis functions include basic statistics, drift, drift removal, normalization, scaling, gap and outlier detection and removal, as well as Allan variance and power spectrum, all over selectable limits with gaps ignored.

Figure 8 a), b) shows the PSD obtained for the first comparison (R_s, 10 TΩ / MI : R_x, 100 TΩ / GdL) at the test voltage of 1000 V (positive and, respectively, negative polarity of R_x) and for the program at a fixed settle time and variable test voltages obtained with the software Stable32 and the raw data TEK00003_FFT and TEK00005_FFT, obtained with the scope.

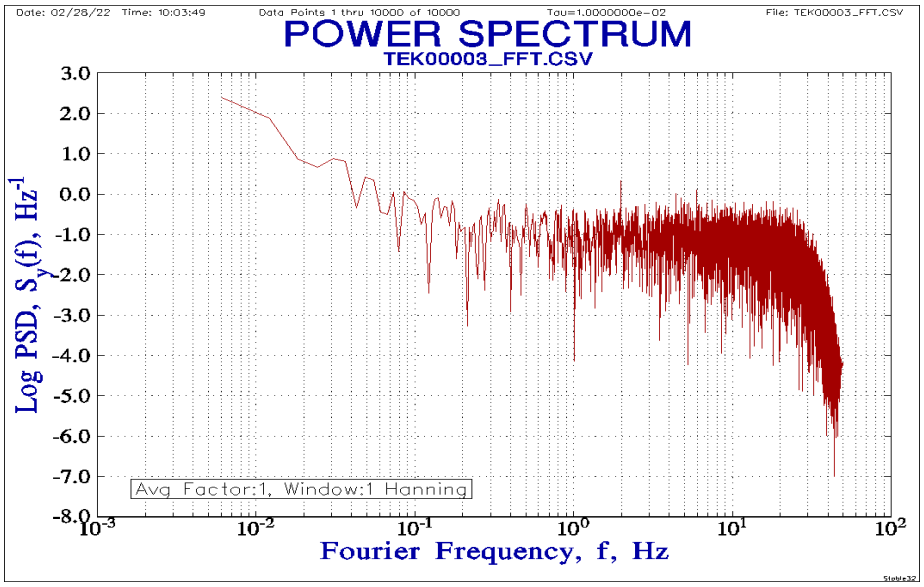

Figure 8 a). PSD obtained for the first comparison at positive polarity of R_x (R_s, 10 TΩ / MI : R_x, 100 TΩ / GdL) and test voltage of 1000 V, in the frequency range from 0 Hz to 50 Hz.

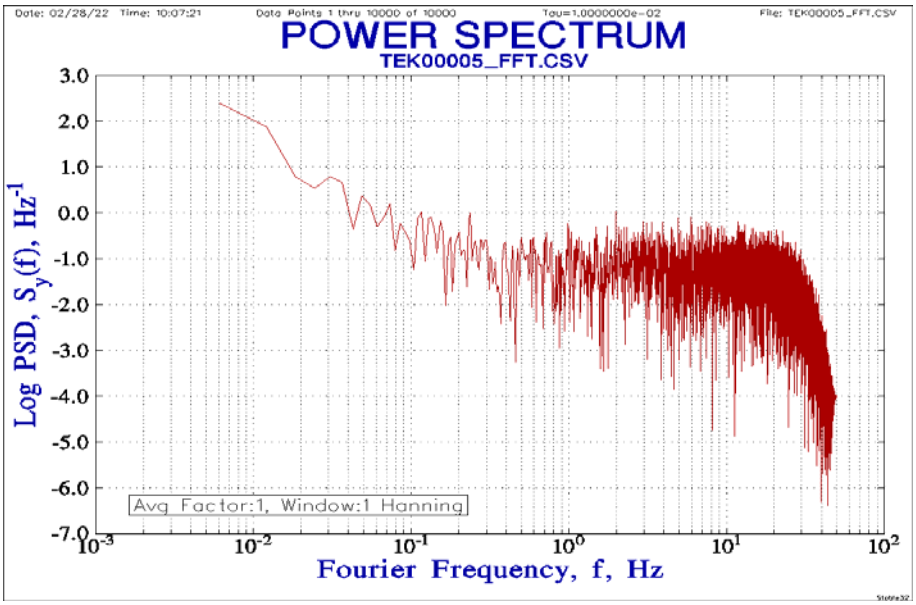

Figure 8 b). PSD obtained for the first comparison at negative polarity (R_s, 10 TΩ / MI : R_x, 100 TΩ / GdL) and test voltage of 1000 V, in the frequency range from 0 Hz to 50 Hz.

Stable32 is also used to compute the Allan variation at the time interval of 0.01 s from the raw data TEK00003_FFT and TEK00005_FFT, obtained with the scope (positive and, respectively, negative polarity of R_x). The results are shown in Figure 9 a) and b).

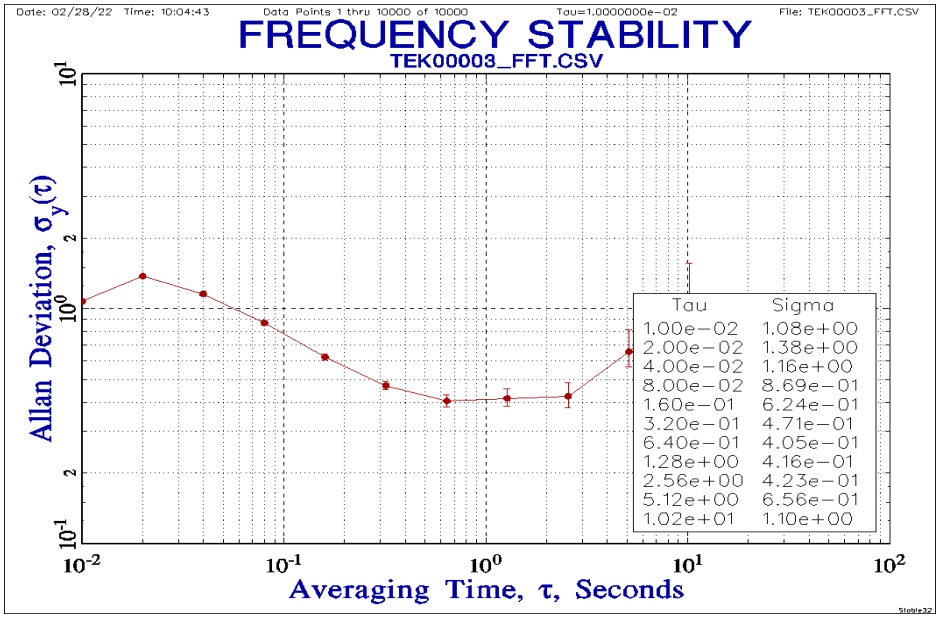

Figure 9 a). Allan deviation obtained from the raw data TEK00003_FFT.

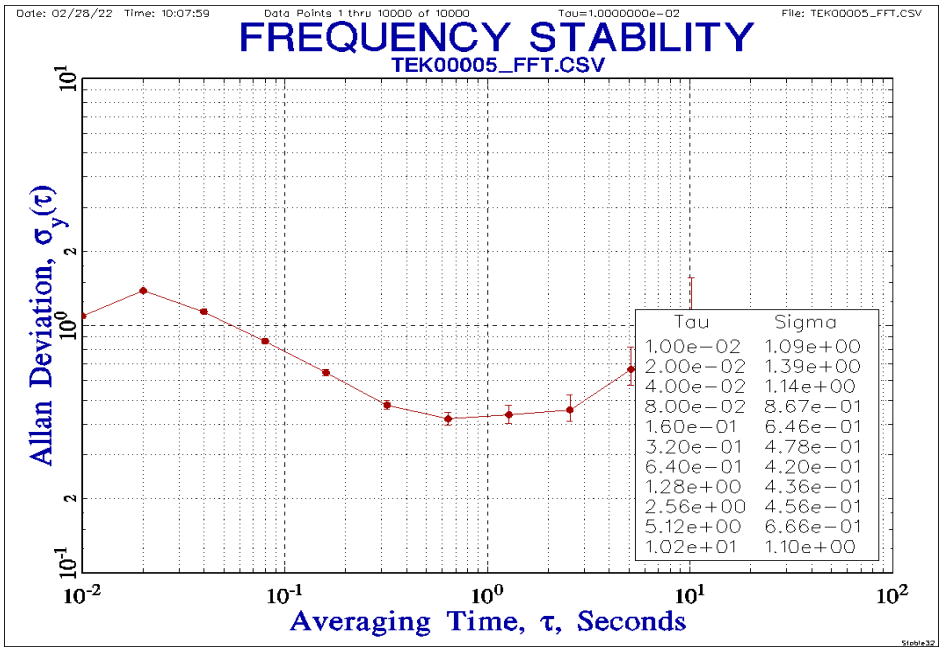

Figure 9 a). Allan deviation obtained from the raw data TEK00005_FFT.

Considering that the detector has a parabola-like shape for its speed vs. noise characteristics and are optimized for the readings rate between 20 ms and 200 ms. At these speeds, the detectors will make corrections for its own internal drift and still be fast enough to settle a step response. The software of the MI 6600A sets the detector at 1 PLC that equals to the readings rate of 20 ms. To obtain the number of electrometer readings to be used for each ratio measurement the averaging time obtained at the minimum value of the Allan deviation is divided by 20 ms. The results for the first comparison (R_s, 10 TΩ / MI : R_x, 100 TΩ / GdL) are shown in Table 7.

Table 7. Conversion from the minimum Allan variation to the number of the electrometer readings for the ratio 1:10.

Test, V	**$\sigma_y(\tau)$, mV**	**τ, s**	***N*, number of electrometer readings (1PLC[(2)] = 20 ms)**
0	0,37	5,12	256[(1)]
250	0,43	1,28	64
500	0,39	0,64	32
750	0,41	0,64	32
1000	0,40	0,64	32

Note: 1) The number of electrometer readings is limited (by the software version 2.2.0) at 100 readings.
DIGITAL FILTER**:** averaging (selectable from 2 to 100 readings).
2) MED — Selects the medium integration time (1 PLC) and sets display resolution to 5½-digit resolution. MED rate is selected when a compromise between noise performance and speed is acceptable.

Measuring for any longer than the optimum measurement time (or the optimum electrometer readings) for the measurement bridge is counterproductive, as the random drift will start to dominate. In addition, failure to correctly treat correlations can produce significant errors in any Type A uncertainty.

3. RATIO COMPARISONS BETWEEN THE RESISTORS OF 10 TΩ AND 100 TΩ

This paragraph reports the experimental results for the ratio measurement comparisons between high value resistors and their resistance reported in Figure 4) and Table 2).

COMPARISON A. (R_S, 10 TΩ / MI : R_X, 100 TΩ / GDL)

The comparison A is the first of the four comparisons from the campaign of measurements done between the beginning of March and end of April.

Table 8a). The ratio program R_S, 10 TΩ / MI : R_x, 100 TΩ / GdL.

Comparison A			Period		Settle-time	Unbal.	Test voltage	Ratio, r	Ratio, r	sdvm
n.	Task		from	to	(s)	(ppm)	(V)		(ppm)	(ppm)
Prog1. with 50 measurements used for statistics for each task										
1	$r_{A0/250\ V}$	3τ	03/03/2022 10:45	04/03/2022 15:23	1800	40001	250	10.2016	20161	693
2	$r_{A0/500\ V}$	3τ	04/03/2022 15:28	05/03/2022 19:25	1800	20001	500	10.1735	17351	406
3	$r_{A0/750\ V}$	3τ	05/03/2022 19:30	06/03/2022 23:27	1800	13334	750	10.1799	17987	344
4	$r_{A0/1000\ V}$	3τ	06/03/2022 23:32	08/03/2022 03:30	1800	10001	1000	10.1755	17551	255
Prog2. with 20 measurements used for statistics for each task										
5	$r_{A1/250\ V}$	1/2τ	08/03/2022 03:35	08/03/2022 06:19	300	40001	250	10.1812	18121	1338
6	$r_{A2/250\ V}$	1τ	08/03/2022 06:24	08/03/2022 11:07	600	-	250	10.2055	20554	1807
7	$r_{A3/250\ V}$	2τ	08/03/2022 11:12	08/03/2022 19:55	1200	-	250	10.1814	18143	**338**
8	$r_{A4/250\ V}$	3τ	08/03/2022 20:00	09/03/2022 08:43	1800	-	250	10.1916	19161	1167
9	$r_{A1/500\ V}$	1/2τ	09/03/2022 08:48	09/03/2022 11:14	300	20001	500	10.1701	17014	604
10	$r_{A2/500\ V}$	1τ	09/03/2022 11:19	09/03/2022 15:44	600	-	500	10.1818	18183	629
11	$r_{A3/500\ V}$	2τ	09/03/2022 15:49	10/03/2022 00:14	1200	-	500	10.1754	17542	**156**
12	$r_{A4/500\ V}$	3τ	10/03/2022 00:19	10/03/2022 12:44	1800	-	500	10.1452	14520	335
13	$r_{A1/750\ V}$	1/2τ	10/03/2022 12:49	10/03/2022 15:15	300	13334	750	10.1730	17299	349

14	$r_{A2/750\ V}$	1τ	10/03/2022 15:20	10/03/2022 19:45	600	-	750	10.1686	16859	298
15	$r_{A3/750\ V}$	2τ	10/03/2022 19:50	11/03/2022 04:16	1200	-	750	10.1752	17524	**91**
16	$r_{A4/750\ V}$	3τ	11/03/2022 13:14	12/03/2022 01:40	1800	-	750	10.1684	16842	496
17	$r_{A1/1000\ V}$	1/2τ	12/03/2022 01:45	12/03/2022 04:11	300	10001	1000	10.1715	17146	311
18	$r_{A2/1000\ V}$	1τ	12/03/2022 04:16	12/03/2022 08:42	600	-	1000	10.1872	18718	197
19	$r_{A3/1000\ V}$	2τ	12/03/2022 08:47	12/03/2022 17:12	1200	-	1000	10.1737	17367	**81**
20	$r_{A4/1000\ V}$	3τ	12/03/2022 17:17	13/03/2022 05:43	1800	-	1000	10.1632	16320	251
Prog1. with 50 measurements used for statistics for each task										
21	$r_{A0/1000\ V}$	3τ	21/04/2022 17:55	22/04/2022 07:30	840	10001	1000	10,1738	17384	193
22	$r_{A0/1000\ V}$	3τ	22/04/2022 07:35	22/04/2022 21:09	840	10001	1000	10,1736	17359	186
Prog2. with 20 measurements used for statistics for each task										
23	$r_{A1/1000\ V}$	1/2τ	22/04/2022 21:14	22/04/2022 22:36	140	10001	1000	10,1710	17098	188
24	$r_{A2/1000\ V}$	1τ	22/04/2022 22:41	23/04/2022 00:59	280	10001	1000	10,1746	17455	248
25	$r_{A3/1000\ V}$	2τ	23/04/2022 01:04	23/04/2022 05:15	560	10001	1000	10,1829	18287	**147**
26	$r_{A4/1000\ V}$	3τ	23/04/2022 05:20	23/04/2022 11:22	840	10001	1000	10,1748	17484	358

In the Table 8a) with blue colour in the last column, the value for the standard deviation of the mean (**sdvm)** is reported as the minimum for each test voltage. The minimum value is obtaned at the third step/ step 3 as a consequence of the iteration and white noise regime described in the previous paragraph, it does not depend on the settle time and it does not depend on the test voltages. In case of program Prog2, the Task from 23 to 26 are performed with a time constant τ equal to 280 s instead of 600 s and the minimum value is also obtained at step 3.

In the Figure 10 it is shown the relative deviation of the measurements at settle time 3τ measuring at constant settle time for Tasks from 1 to 4 of program Prog1 compared with the

measurements at Tasks 8, 12, 16 and 20 of program Prog2. The reasons of these deviations shown in Figure 10 will be further investigated in accordance with the manufacturer.

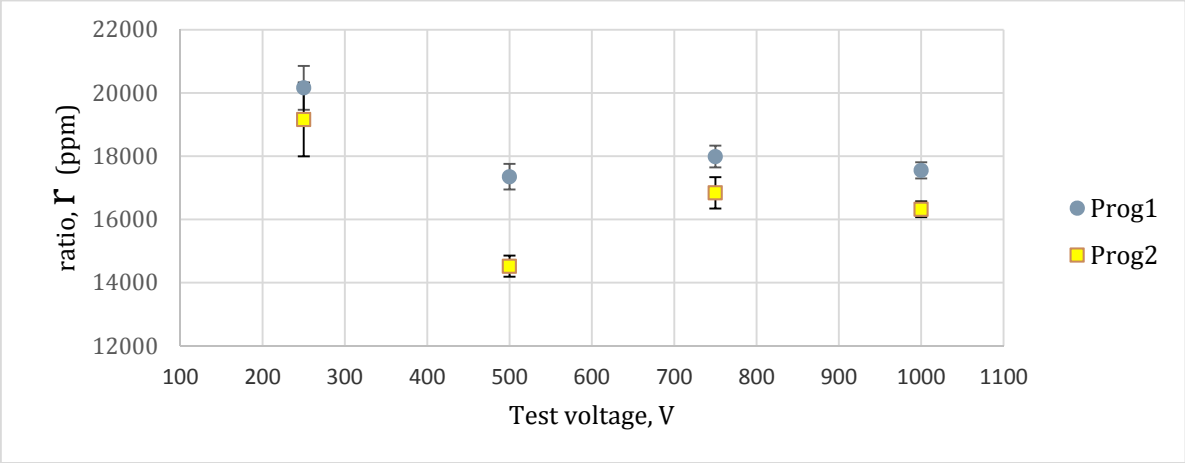

Figure 10. Relative deviation of the measurements at settle time 3τ measuring at constant settle time (blue dots) and with autoupdate (yellow dots).

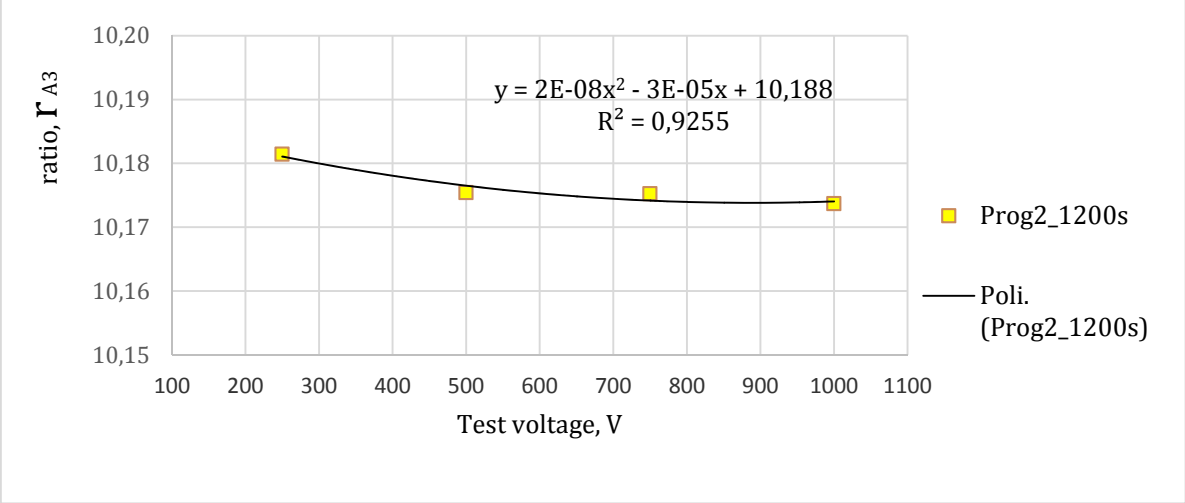

Figure 11. The ratio measurements at settle time 2τ measuring with autoupdate and its polinomial iterpolation.

The Figure 10 and Figure 11 shows a different behavior for the ratio in case of step 3 and step 4 of the program Prog2.

Using the Sturges rule for the histograms, $\boldsymbol{b = 1 + 3{,}322 * \log(N)}$, where $\boldsymbol{b}$ is the number of bins and N is the number of measurements (50 for Prog1 and 20 for Prog2) in case of the test at 1000 V for the comparison A it is obtained the histograms shown in figures from 12 to 15.

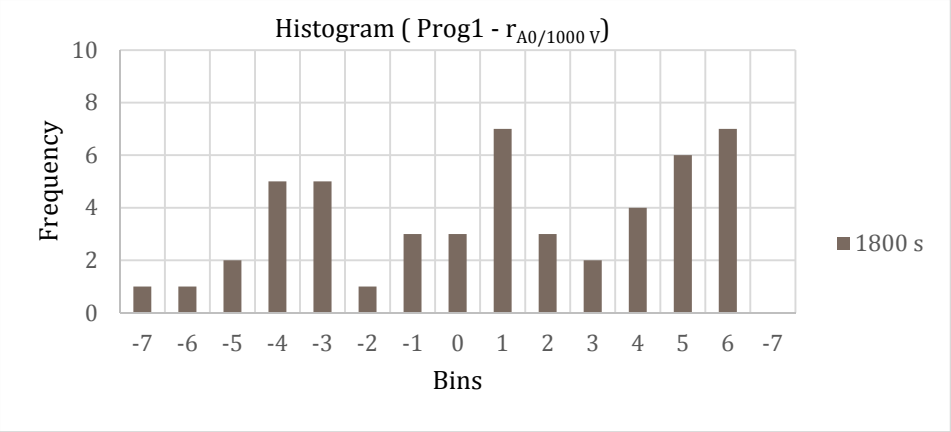

Figure 12. The histogram for the program Prog1 at 1000 V for the ratio measurements at constant settle time of 1800 s.

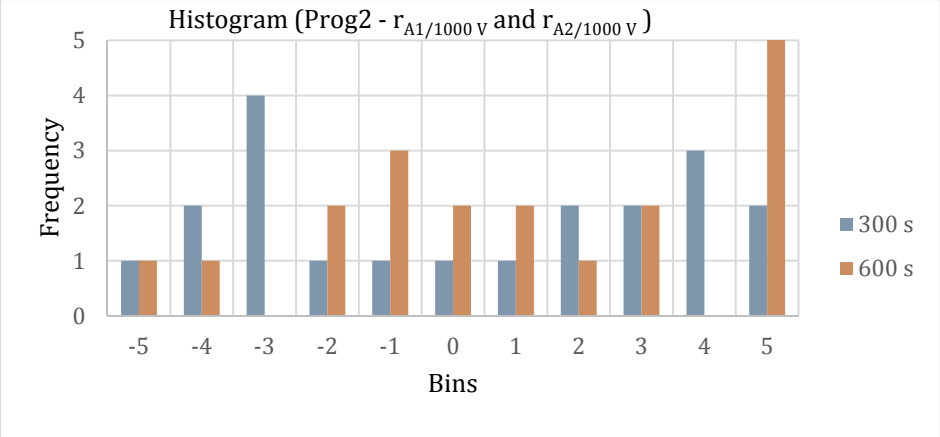

Figure 13. The histogram for the program Prog2 at 1000 V for the ratio measurements at settle time of 300 s and 600 s.

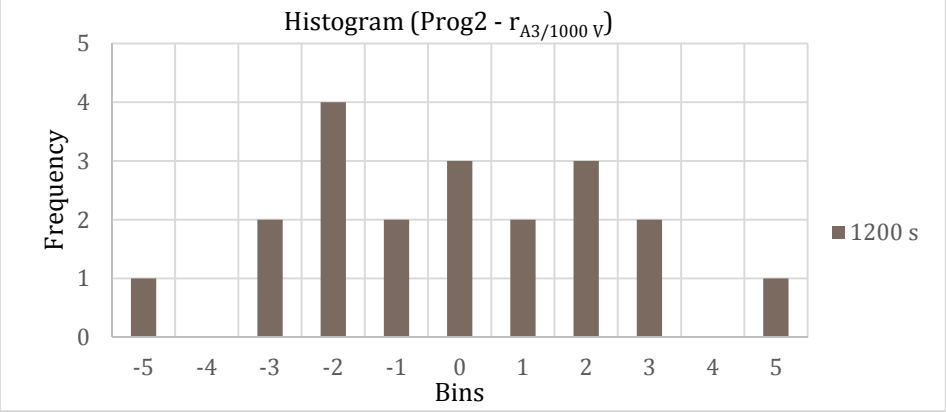

Figure 14. The histogram for the program Prog2 at 1000 V for the ratio measurements at settle time of 1200 s / step 3.

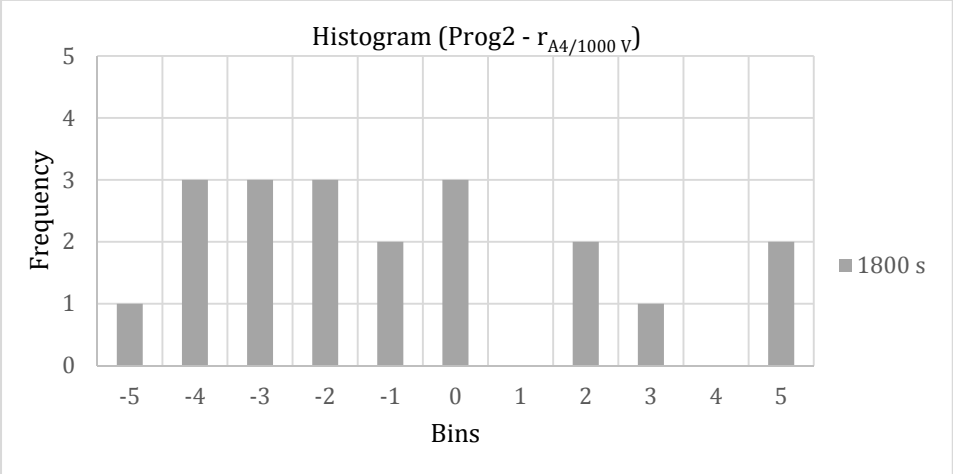

Figure 15. The histogram for the program Prog2 at 1000 V for the ratio measurements at settle time of 1800 s.

COMPARISON B. (R_S, 10 TΩ / MI : R_X, 100 TΩ / MI)

The comparison B is the second of the four comparisons from the campaign of measurements.

Table 8b). The ratio program R_s, 10 TΩ / MI : R_x, 100 TΩ / MI

Comparison B			Period		Settle-time	Unbal.	Test voltage	Ratio, r	Ratio, r	sdvm
n.	Task		from	to	(s)	(ppm)	(V)		(ppm)	(ppm)
Prog1. with 50 measurements used for statistics for each task										
1	$r_{B0/250\ V}$	3τ	14/03/2022 11:12	15/03/2022 15:49	1800	40001	250	10.0324	3241	897
2	$r_{B0/500\ V}$	3τ	15/03/2022 15:54	16/03/2022 20:22	1800	20001	500	9.7793	-22066	317
3	$r_{B0/750\ V}$	3τ	16/03/2022 20:27	18/03/2022 00:56	1800	13334	750	9.5459	-45410	254
4	$r_{B0/1000\ V}$	3τ	18/03/2022 01:01	19/03/2022 05:31	1800	10001	1000	9.3265	-67354	167
Prog2. with 20 measurements used for statistics for each task										
5	$r_{B1/250\ V}$	1/2τ	19/03/2022 05:36	19/03/2022 08:19	300	40001	250	10.0100	998	1476
6	$r_{B2/250\ V}$	1τ	19/03/2022 08:24	19/03/2022 13:08	600	-	250	10.0447	4470	664
7	$r_{B3/250\ V}$	2τ	19/03/2022 13:13	19/03/2022 21:56	1200	-	250	10.0293	2929	**440**
8	$r_{B4/250\ V}$	3τ	19/03/2022 22:01	20/03/2022 10:45	1800	-	250	9.9767	-2327	574

9	$r_{B1/500\ V}$	1/2τ	20/03/2022 10:50	20/03/2022 13:21	300	20001	500	9.7469	-25305	278
10	$r_{B2/500\ V}$	1τ	20/03/2022 13:26	20/03/2022 17:52	600	-	500	9.7439	-25612	467
11	$r_{B3/500\ V}$	2τ	20/03/2022 17:57	21/03/2022 02:22	1200	-	500	9.7607	-23928	**211**
12	$r_{B4/500\ V}$	3τ	21/03/2022 02:27	21/03/2022 14:53	1800	-	500	9.7742	-22583	518
13	$r_{B1/750\ V}$	1/2τ	21/03/2022 14:58	21/03/2022 17:30	300	13334	750	9.5140	-48597	299
14	$r_{B2/750\ V}$	1τ	21/03/2022 17:35	21/03/2022 22:00	600	-	750	9.5256	-47444	312
15	$r_{B3/750\ V}$	2τ	21/03/2022 22:05	22/03/2022 06:31	1200	-	750	9.5332	-46677	**163**
16	$r_{B4/750\ V}$	3τ	22/03/2022 06:36	22/03/2022 19:02	1800	-	750	9.5384	-46163	232
17	$r_{B1/1000\ V}$	1/2τ	22/03/2022 19:07	22/03/2022 21:39	300	10001	1000	9.3148	-68525	275
18	$r_{B2/1000\ V}$	1τ	22/03/2022 21:44	23/03/202 2 02:10	600	10001	1000	9.3206	-67945	272
19	$r_{B3/1000\ V}$	2τ	23/03/2022 02:15	23/03/202 2 10:42	1200	10001	1000	9.3320	-66804	**134**
20	$r_{B4/1000\ V}$	3τ	23/03/2022 10:47	23/03/202 2 23:13	1800	10001	1000	9.3335	-66650	205

In the Table 8b) with blue color in the last column, the value for the standard deviation of the mean (**sdvm),** is reported as the minimum for each test voltage. Also in this comparison, the minimum value is obtaned at the third step / step 3 as a consegence of the iteration and white noise regime, it does not depend on the settle time.

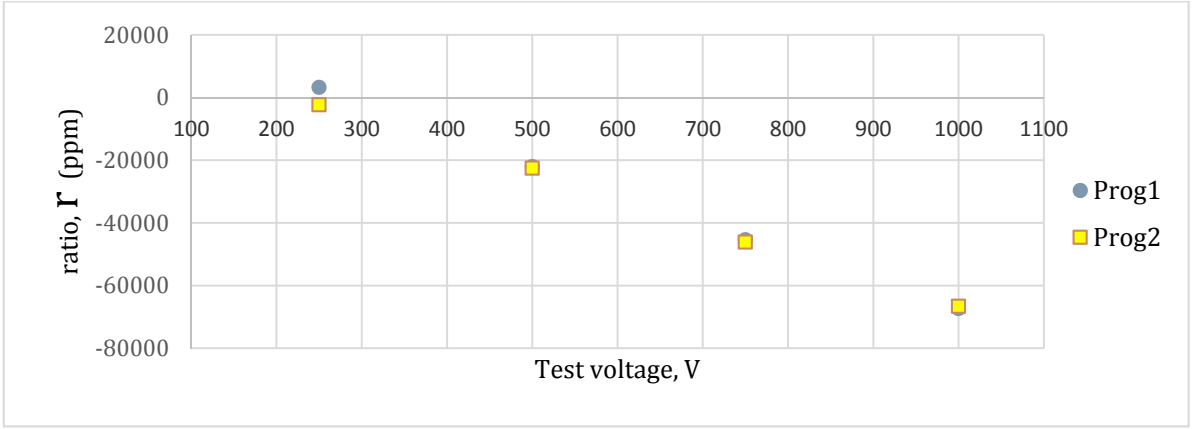

Figure 16. Relative deviation of the measurements at settle time 3τ measuring at a constant settle time (blue dots) in Prog1 and with autoupdate (yellow dots) in Prog2. (the uncertainties are less than the dots and it can't be shown).

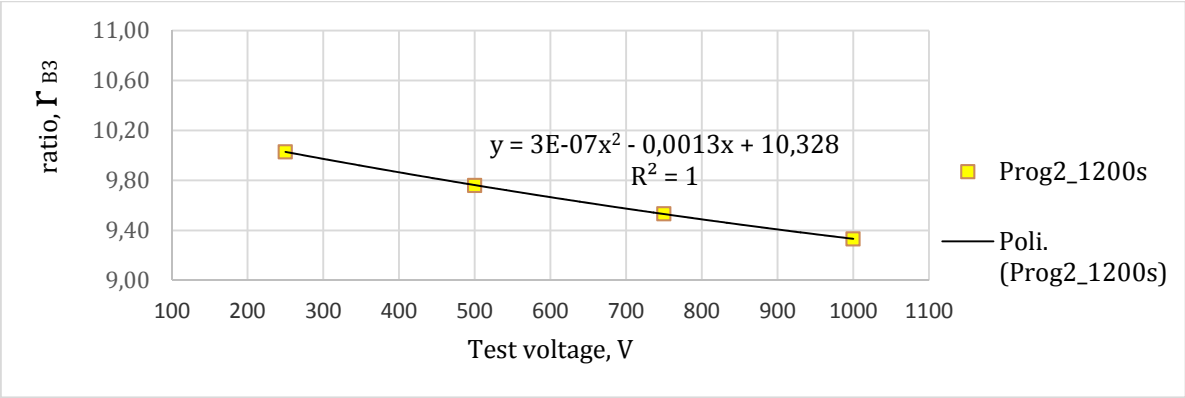

Figure 17. The ratio measurements at settle time 2τ measuring with autoupdate and its polinomial iterpolation.

In case of the test at 1000 V for the comparison B the histograms are shown in figures from 18 to 21.

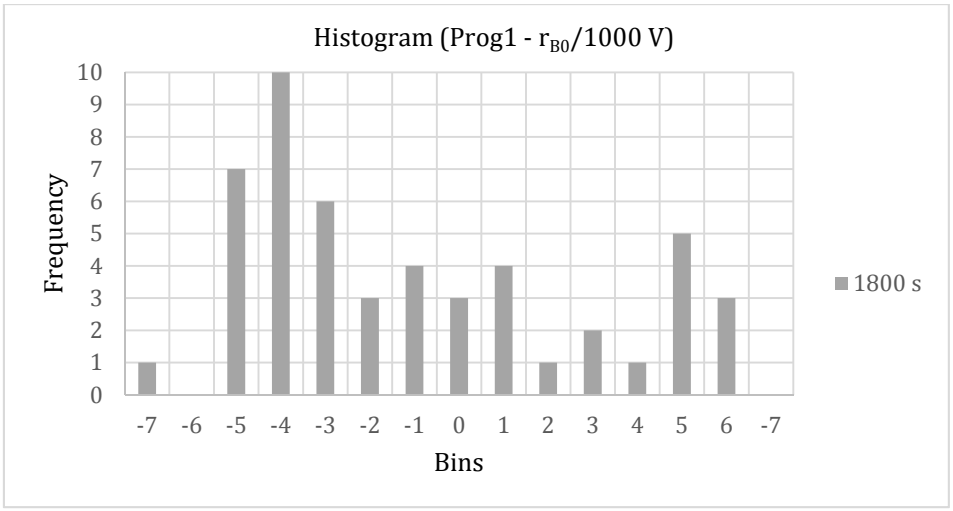

Figure 18. The histogram for the program Prog1 at 1000 V for the ratio measurements at constant settle time of 1800 s.

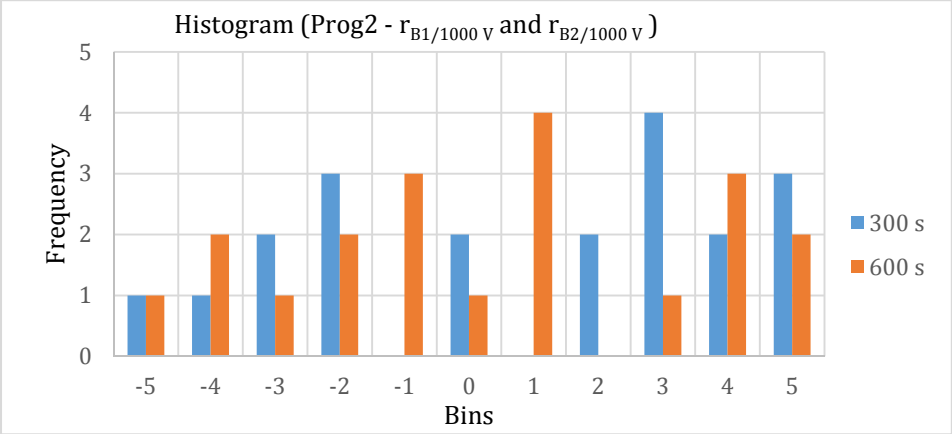

Figure 19. The histogram for the program Prog2 at 1000 V for the ratio measurements at settle time of 300 s and 600 s.

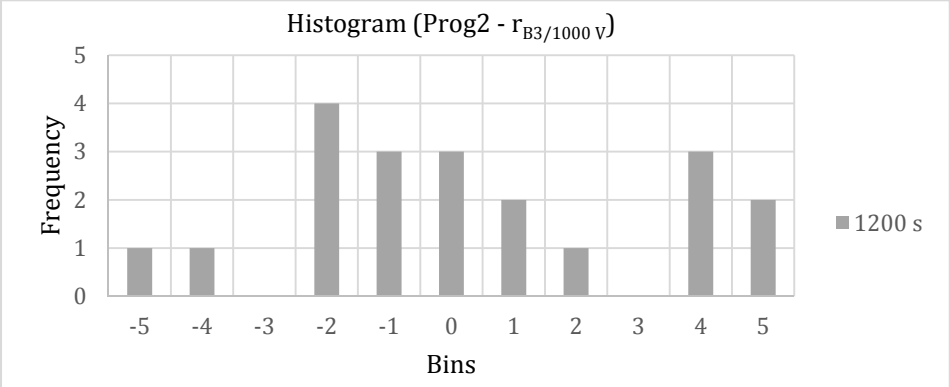

Figure 20. The histogram for the program Prog2 at 1000 V for the ratio measurements at settle time of 1200 s / step 3.

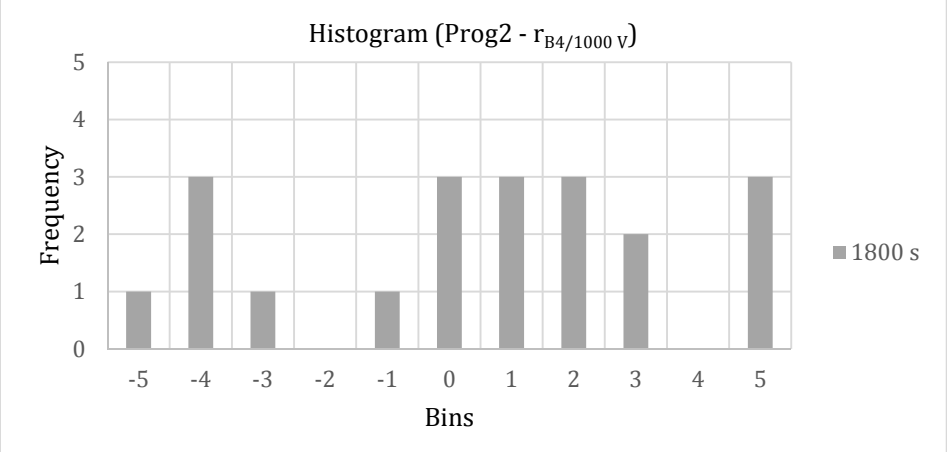

Figure 21. The histogram for the program Prog2 at 1000 V for the ratio measurements at settle time of 1800 s.

COMPARISON C. (R_S, 100 TΩ / MI : R_X, 100 TΩ / GdL)

The comparison C is the third of the four comparisons from the campaign of measurements.

Table 8c). The ratio program R_s, 100 TΩ / MI : R_x, 100 TΩ / GdL

Comparison C			Period		Settle-time	Unbal.	Test voltage	Ratio, r	Ratio, r	sdvm
n.	Task		from	to	(s)	(ppm)	(V)		(ppm)	(ppm)
Prog1. with 50 measurements used for statistics for each task										
1	$r_{C0/250\ V}$	3τ	24/03/2022 16:09	25/03/2022 20:48	1800	40001	250	1.0138	13809	607
2	$r_{C0/500\ V}$	3τ	25/03/2022 20:53	27/03/2022 01:24	1800	20001	500	1.0399	39867	289
3	$r_{C0/750\ V}$	3τ	27/03/2022 01:29	28/03/2022 06:59	1800	13334	750	1.0605	60529	198
4	$r_{C0/1000\ V}$	3τ	28/03/2022 07:04	29/03/2022 12:06	1800	10001	1000	1.0829	82876	142
Prog2. (R_s, 100 TΩ / MI : R_x, 100 TΩ / GdL) with 20 measurements used for statistics for each task										
5	$r_{C1/250\ V}$	1/2τ	29/03/2022 12:11	29/03/2022 14:56	300	40001	250	1.0168	16765	736
6	$r_{C2/250\ V}$	1τ	29/03/2022 15:01	29/03/2022 19:45	600	-	250	1.0158	15785	939
7	$r_{C3/250\ V}$	2τ	29/03/2022 19:50	30/03/2022 04:35	1200	-	250	1.0146	14613	**464**
8	$r_{C4/250\ V}$	3τ	30/03/2022 04:40	30/03/2022 17:24	1800	-	250	1.0154	15374	688
9	$r_{C1/500\ V}$	1/2τ	30/03/2022 17:29	30/03/2022 20:02	300	20001	500	1.0404	40439	353
10	$r_{C2/500\ V}$	1τ	30/03/2022 20:07	31/03/2022 00:33	600	-	500	1.0408	40833	641
11	$r_{C3/500\ V}$	2τ	31/03/2022 00:38	31/03/2022 09:05	1200	-	500	1.0404	40350	**256**
12	$r_{C4/500\ V}$	3τ	31/03/2022 09:10	31/03/2022 21:37	1800	-	500	1.0410	40987	549
13	$r_{C1/750\ V}$	1/2τ	31/03/2022 21:42	01/04/2022 00:14	300	13334	750	1.0633	63297	268
14	$r_{C2/750\ V}$	1τ	01/04/2022 00:19	01/04/2022 04:46	600	-	750	1.0645	64528	409
15	$r_{C3/750\ V}$	2τ	01/04/2022 04:51	01/04/2022 13:18	1200	-	750	1.0629	62945	**188**
16	$r_{C4/750\ V}$	3τ	01/04/2022 13:23	02/04/2022 01:49	1800	-	750	1.0638	63842	255
17	$r_{C1/1000\ V}$	1/2τ	02/04/2022 01:54	02/04/2022 04:33	300	10001	1000	1.0846	84601	248
18	$r_{C2/1000\ V}$	1τ	02/04/2022 04:38	02/04/2022 09:05	600	-	1000	1.0849	84901	355

19	$r_{C3/1000\ V}$	2τ	02/04/2022 09:10	02/04/2022 17:37	1200	-	1000	1.0837	83689	**137**
20	$r_{C4/1000\ V}$	3τ	02/04/2022 17:42	03/04/2022 06:09	1800	-	1000	1.0836	83597	318

In the Table 8c) with blue color in the last column, the value for the standard deviation of the mean (**sdvm),** is reported as the minimum for each test voltage. Also in this comparison, the minimum value is obtaned at the third step / step 3 as a consegence of the iteration and white noise regime and does not depend on the settle time and it does not depend on the ratio 1:1 or 1:10.

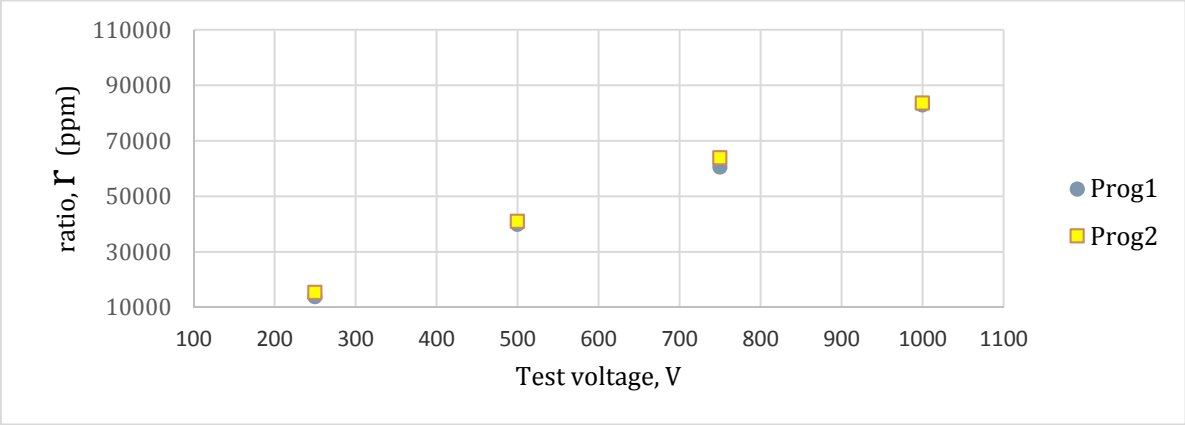

Figure 22. Relative deviation of the measurements at settle time 3τ measuring at constant settle time (blue dots) in Prog1 and with autoupdate (yellow dots) in Prog2. (the uncertainties are less than the dots and it can't be shown).

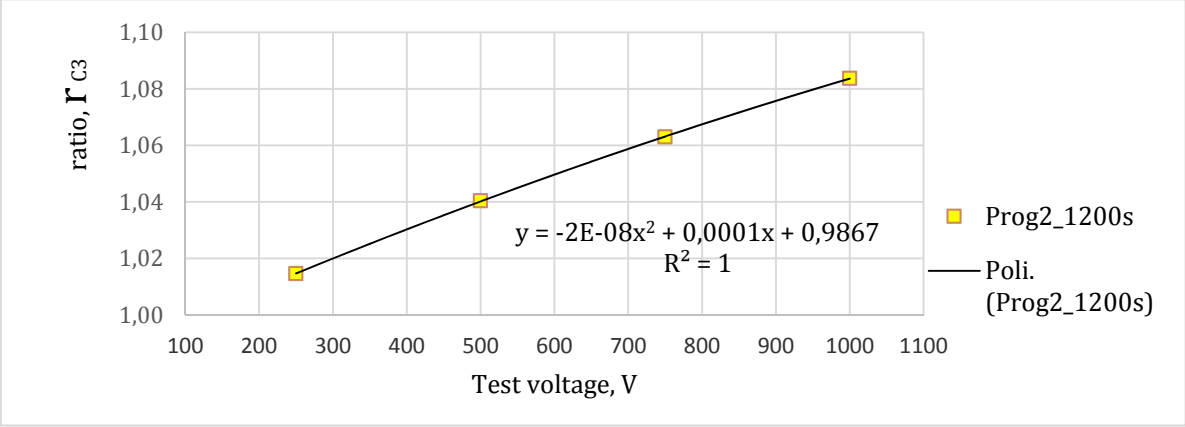

Figure 23. The ratio measurements at settle time 2τ measuring step 3 with autoupdate and its polinomial iterpolation.

In case of the test at 1000 V for the comparison C the histograms are shown in figures from 24 to 26.

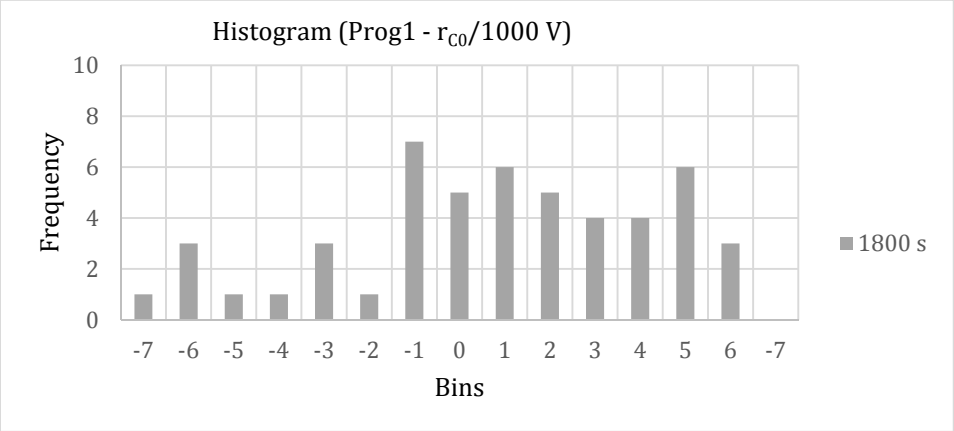

Figure 24. The histogram for the program Prog1 at 1000 V for the ratio measurements at constant settle time of 1800 s.

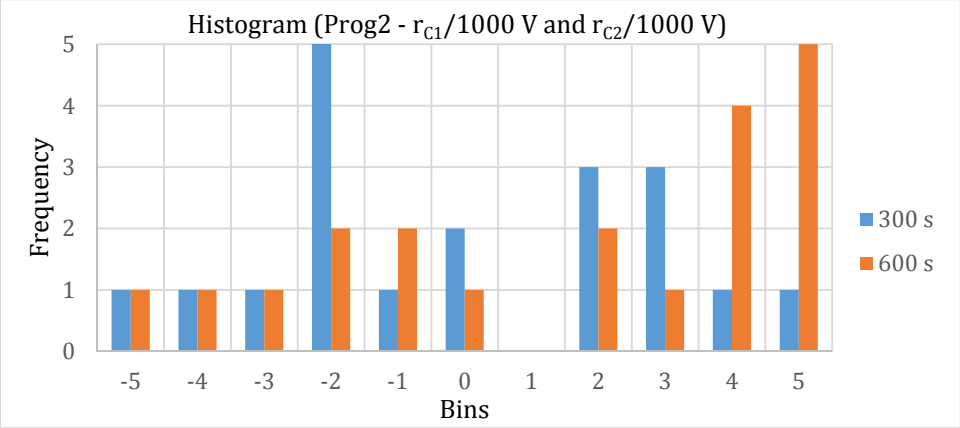

Figure 25. The histogram for the program Prog2 at 1000 V for the ratio measurements at settle time of 300 s and 600 s.

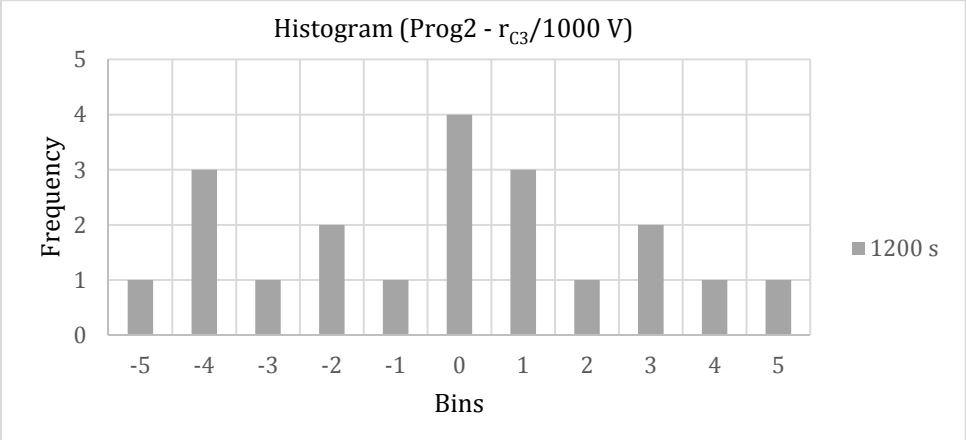

Figure 26. The histogram for the program Prog2 at 1000 V for the ratio measurements at settle time of 1200 s / step 3.

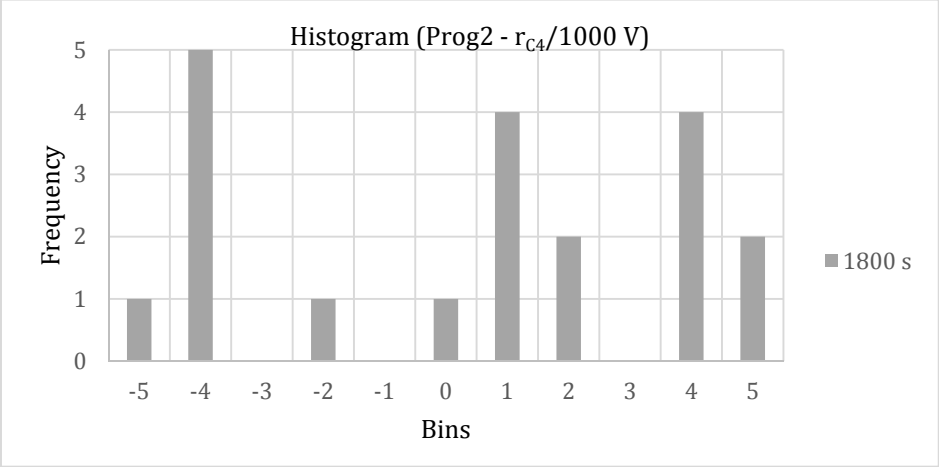

Figure 27. The histogram for the program Prog2 at 1000 V for the ratio measurements at settle time of 1800 s.

COMPARISON D. (R_S, 100 TΩ / GdL : R_X, 100 TΩ / MI)

The comparison D is the last comparisons from the campaign of measurements.

Table 8d). The ratio program R_s, 100 TΩ / GDl : R_x, 100 TΩ / MI

Comparison D			Period		Settle-time	Unbal.	Test voltage	Ratio, r	Ratio, r	sdvm
n.	Task		from	to	(s)	(ppm)	(V)		(ppm)	(ppm)
Prog1. with 50 measurements used for statistics for each task										
1	$r_{D0/250\ V}$	3τ	04/04/2022 10:09	05/04/2022 14:49	1800	40001	250	0.9863	-13708	765

2	$r_{D0/500\ V}$	3τ	05/04/2022 14:54	06/04/2022 19:24	1800	20001	500	0.9597	-40297	271
3	$r_{D0/750\ V}$	3τ	06/04/2022 19:29	08/04/2022 00:00	1800	13334	750	0.9372	-62772	182
4	$r_{D0/1000\ V}$	3τ	08/04/2022 00:05	09/04/2022 08:45	1800	10001	1000	0.9171	-82868	93
Prog2. with 20 measurements used for statistics for each task										
5	$r_{D1/250\ V}$	1/2τ	09/04/2022 08:50	09/04/2022 11:34	300	40001	250	0.9840	-15955	508
6	$r_{D2/250\ V}$	1τ	09/04/2022 11:39	09/04/2022 16:23	600	-	250	0.9845	-15523	681
7	$r_{D3/250\ V}$	2τ	09/04/2022 16:28	10/04/2022 01:12	1200	-	250	0.9856	-14373	**409**
8	$r_{D4/250\ V}$	3τ	10/04/2022 01:17	10/04/2022 14:02	1800	-	250	0.9856	-14364	659
9	$r_{D1/500\ V}$	1/2τ	10/04/2022 14:07	10/04/2022 16:39	300	20001	500	0.9576	-42361	276
10	$r_{D2/500\ V}$	1τ	10/04/2022 16:44	10/04/2022 21:11	600	-	500	0.9594	-40639	507
11	$r_{D3/500\ V}$	2τ	10/04/2022 21:16	11/04/2022 05:43	1200	-	500	0.9593	-40733	**153**
12	$r_{D4/500\ V}$	3τ	11/04/2022 05:48	11/04/2022 18:14	1800	-	500	0.9606	-39386	320
13	$r_{D1/750\ V}$	1/2τ	11/04/2022 18:19	11/04/2022 20:52	300	13334	750	0.9350	-65004	199
14	$r_{D2/750\ V}$	1τ	11/04/2022 20:57	12/04/2022 01:23	600	-	750	0.9363	-63706	230
15	$r_{D3/750\ V}$	2τ	12/04/2022 01:28	12/04/2022 09:54	1200	-	750	0.9367	-63253	**143**
16	$r_{D4/750\ V}$	3τ	12/04/2022 09:59	12/04/2022 22:26	1800	-	750	0.9372	-62829	205
17	$r_{D1/1000\ V}$	1/2τ	12/04/2022 22:31	13/04/2022 01:52	300	10001	1000	0.9151	-84851	170
18	$r_{D2/1000\ V}$	1τ	Out of range for the voltage Vs							
19	$r_{D3/1000\ V}$	2τ	Out of range for the voltage Vs							
20	$r_{D4/1000\ V}$	3τ	Out of range for the voltage Vs							

In the Table 8d) with blue colour in the last column, the value for the standard deviation of the mean (**sdvm)** is reported as the minimum for each test voltage. Also in this comparison, the minimum value is obtained at the third step / step 3 as a consegence of the iteration and white noise regime and does not depend on the settle time (except the last 3 tasks). The tasks from 18 to 20 were not perfomed because the voltage S2 on low part of the bridge was higher than 1050 V and the program was out of range.

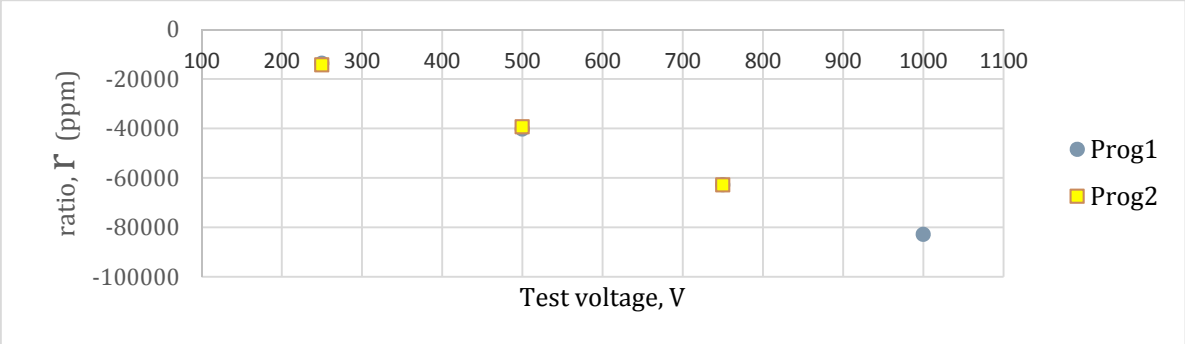

Figure 28. Relative deviation of the measurements at settle time 3τ measuring at constant settle time (blue dots) in Prog1 and with autoupdate (yellow dots) in Prog2. (the uncertainties are less than the dots and it can't be shown). The measurements at 1000 V for the Prog2 was not performed by the bridge.

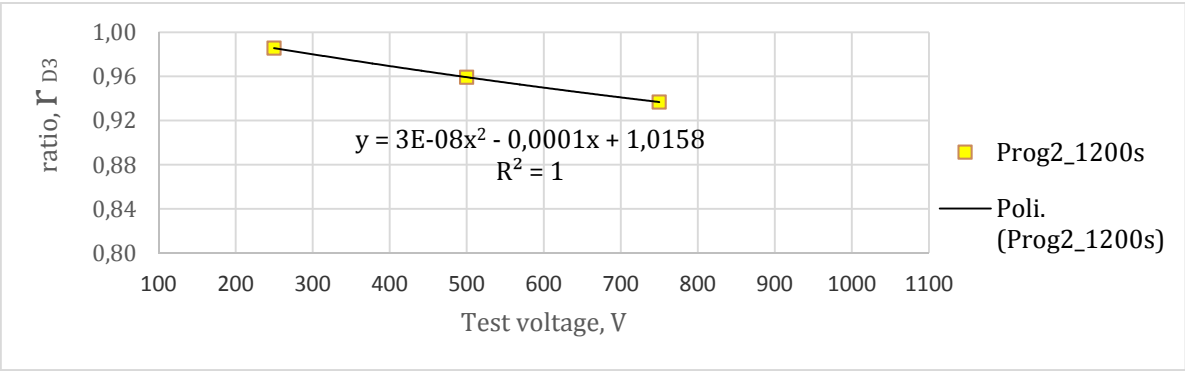

Figure 29. The ratio measurements at settle time 2τ measuring step 3 with autoupdate and its polinomial iterpolation. The measurements at 1000 V for the Prog2 are not performed.

In case of the test at 1000 V for the comparison C the histograms are shown in figures from 30 to 31.

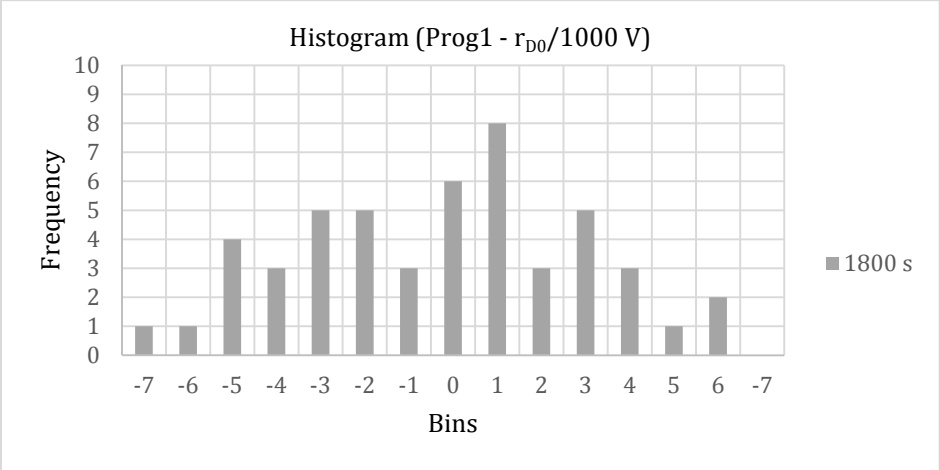

Figure 30. The histogram for the program Prog1 at 1000 V for the ratio measurements at constant settle time of 1800 s.

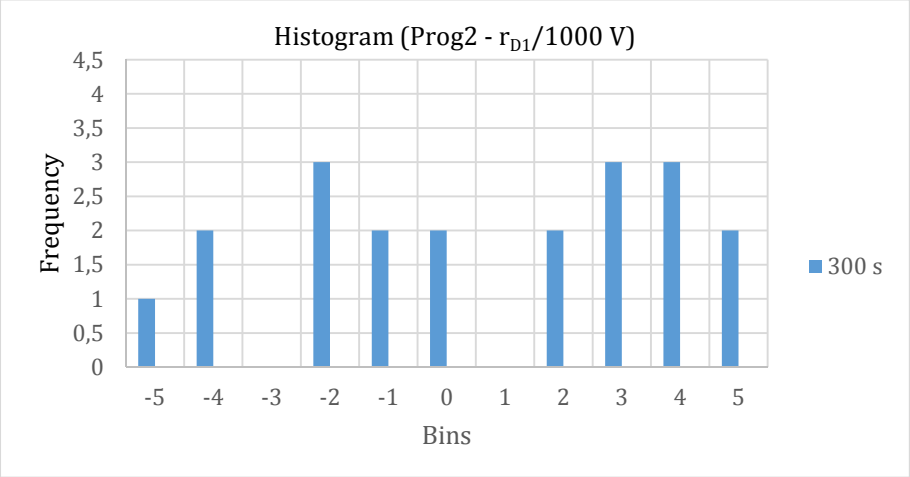

Figure 31. The histogram for the program Prog2 at 1000 V for the ratio measurements at settle time of 300 s.

4. WHY TRIANGULATIONS RULES?

These metrological triangulation rules can be used to reduce the systematic errors when using high standard resistance bridge and so to improve the uncertainty of the measurand as in case of calibration or comparisons. Also, this rule can help to understand why the compatibility test is not totally satisfactory as hard measurement noises and instabilities have been detected in particular at 1 PΩ where the compatibility has not yet been achieved [12].

In order to achieve the metrological triangulation rules, it can be accepted the more shrinking condition of both equation 5a) and equation 5b):

$$\left(1-\frac{\overline{r_A}}{\overline{r_B}\cdot\overline{r_C}}\right)\cdot 10^6 < \sqrt[2]{u_{rA}^2+u_{rB}^2+u_{rc}^2}$$

And

$$\left(1-\frac{\overline{r_A}\cdot\overline{r_D}}{\overline{r_B}}\right)\cdot 10^6 < \sqrt[2]{u_{rA}^2+u_{rB}^2+u_{rD}^2}$$

In the Table 9a) and 9b) it is reported the result obtained for these conditions. The green colour indicates the values in agreement with the metrological triangle conditions from equations 5a) and 5b). Only for the test voltage at 250 V, program Prog2 at step 3 was obtained this condition.

Table 9a). The metrological triangulation in case of the condition of the equations 5a).

Comparison	Settle-time		Unbal.	Test voltage	Equations 5a)	RSS
n.		(s)	(ppm)	(V)	(ppm)	(ppm)
Prog1						
1	3τ	1800	40001	250	-3015	1286
2	3τ	1800	20001	500	-422	590
3	3τ	1800	13334	750	-5549	472
4	3τ	1800	10001	1000	-7536	336
Prog2						

5	1/2τ	300	40001	250	-336	2123
6	1τ	600	-	250	-223	2142
7	2τ	1200	-	250	**-549**	**723**
8	3τ	1800	-	250	-6071	1471
9	1/2τ	300	20001	500	-2863	753
10	1τ	600	-	500	-3952	1012
11	2τ	1200	-	500	-2053	366
12	3τ	1800	-	500	2908	825
13	1/2τ	300	13334	750	-5610	532
14	1τ	600	-	750	-2797	594
15	2τ	1200	-	750	-4139	265
16	3τ	1800	-	750	-2079	604
17	1/2τ	300	10001	1000	-6798	484
18	1τ	600	-	1000	-7446	489
19	2τ	1200	-	1000	-6006	208
20	3τ	1800	-	1000	-4890	454

Table 9b). The metrological triangulation in case of the condition of the equations 5b).

Comparison	**Settle-time**		**Unbal.**	**Test voltage**	**Equations 5b)**	**RSS**
n.		(s)	(ppm)	(V)	(ppm)	(ppm)
Prog1						
1	3τ	1800	40001	250	-2927	1368
2	3τ	1800	20001	500	1615	582
3	3τ	1800	13334	750	528	465
4	3τ	1800	10001	1000	-625	319
Prog2						
5	1/2τ	300	40001	250	-878	2056

6	1τ	600	-	250	-240	2042
7	2τ	1200	-	250	**-579**	**689**
8	3τ	1800	-	250	-6865	1458
9	1/2τ	300	20001	500	783	720
10	1τ	600	-	500	-2480	933
11	2τ	1200	-	500	**-23**	**303**
12	3τ	1800	-	500	2921	695
13	1/2τ	300	13334	750	244	501
14	1τ	600	-	750	501	489
15	2τ	1200	-	750	**168**	**235**
16	3τ	1800	-	750	925	585
17	1/2τ	300	10001	1000	682	448
18	1τ	600	-	1000	Out of range for the voltage Vs	
19	2τ	1200	-	1000	Out of range for the voltage Vs	
20	3τ	1800	-	1000	Out of range for the voltage Vs	

In the case of the first condition, the ratios $\bar{r}_A, \bar{r}_B, \bar{r}_C$ are used and in the second case the ratios $\bar{r}_A, \bar{r}_B, \bar{r}_D$ are used, therefore the ratios $\bar{r}_A, \bar{r}_B$ are used for both conditions. The ratio $\bar{r}_C$ obtained by the comparison C between the resistors R_s, 100 TΩ / MI : R_x, 100 TΩ / Gdl is not compatible with the ratio $\bar{r}_D$ obtained by the comparison D between the resistors R_s, 100 TΩ / Gdl : R_x, 100 TΩ / MI: a systematic error of interchangeability of the ratio 1:1 can be the reason of this disagreement.

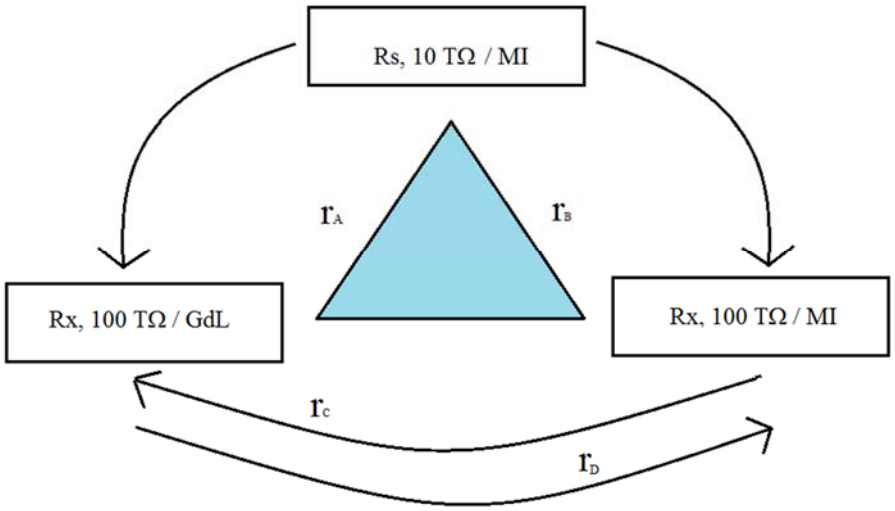

In the case of the comparison D, the value $r_{D2/1000\,V}$, $r_{D3/1000\,V}$ and $r_{D4/1000\,V}$, the measurements at 1000 V for the Prog2, was not performed by the bridge because of the the voltage Vs on S_2 was out of range and higher than 1050 V, the maximum value suppied by the calibrators. In case of the comparison C at 250 V it was obtained the condition of the equation 5a) but not for the other test voltages.

Considering only the partial metrological triangulation of the equation 5b) it can be observed that for the test voltages at 250 V, 500 V and 750 V at step 3 this condition is in ageement and it is less than their corespective RSS. It may also be that the test voltage at 1000 V on step 3 could be in ageement however, it is necessary to reduce the test voltage to 950 V instead of 1000 V.

5. CONCLUSION

Analyzing the metrological triangulation rules applied to the commercial bridge 6600A, currently the best one for ultra-high resistance values seems to be the Multiple Measurement mode with autoupdate function with a measurement process consisting in multiple sessions at increased steps for balancing of the bridge. On the other hand, the long lasting measure steps than the third step could lead to a higher uncertainty for the increasing of the measurements spread due to the oscillating of the regulation balance.

As it can be observed in the next table, the step 3 is also the step where the standard deviation of the mean achieve its minimum value for the ratio R_s, 100 TΩ / Ml : R_x, 1 PΩ / GdL.

All the measurement are grouped and saved in the file **10TMI_100TGdL_100TMI_1PGdL.xls**

Table 10. The ratio program R_s, 100 TΩ / Ml : R_x, 1 PΩ / GdL

Comparison D			Period		Settle-time	Unbal.	Test voltage	Ratio, r	Ratio, r	sdvm
n.	Task		from	to	(s)	(ppm)	(V)		(ppm)	(ppm)
Prog1. with 50 measurements used for statistics for each task										
1	$r_{0/1000\ V}$	3τ	04/05/2022 14:57	05/05/2022 18:56	1800	100001	1000	10.0253	2531	2001
Prog2. with 20 measurements used for statistics for each task										
2	$r_{1/1000\ V}$	1/2τ	05/05/2022 19:01	05/05/2022 21:28	300	100001	1000	10,0729	7291	2935
3	$r_{2/1000\ V}$	1τ	05/05/2022 21:33	06/05/2022 01:59	600	-	1000	10,0257	2569	4174
4	$r_{3/1000\ V}$	2τ	06/05/2022 02:04	06/05/2022 10:30	1200	-	1000	10,0273	2727	**1008**
5	$r_{4/1000\ V}$	3τ	06/05/2022 10:35	06/05/2022 23:02	1800	-	1000	10,2082	20824	1432

Future aims of the work will be the implementation of a triangular ratio test consisting, besides the comparison of the 100 TΩ MI resistor vs. the 100 TΩ Gdl resistor at 250 V, 500 V, 750 V and 950 V and a comparison between a 10 TΩ, 100 TΩ and a 1 PΩ Gdl resistors both resistance network based, to verify the metrological triangulation rules.

BIBLIOGRAPHY

[1] Model 6514 System Electrometer Instruction Manual 4th rev, May 2003

[2] Measurement International, “Automated dual source high resistance bridge model 6600A, operator manual,”, Rev. 5, August 2019

[3] Transmille 3000A Series Precision Multi Product Calibrator Revision No: 1.0, 2006

[4] Mihai I., Galliana F. “Ponte automatico per elevate resistenze in corrente continua MI 6600A: modalità di utilizzo ed approfondimento delle condizioni di misura” RT-2021-02, 2021

[5] Mihai I., “Statistical tools for analysis of the performance of a high resistance measurement bridge” RT-2021-05, 2021

[6] Mihai I., Francese C., "Allestimento del laboratorio Cp107 per misure in corrente continua di alto valore di resistenza elettrica." R.T. 16/2021, 2021

[7] Mihai I. and Marullo Reedtz G. “Using spectral analysis and Allan variance to characterize a potentiometric measurement system.” Proceedings Conf. Celebrating the 50th anniversary of the Romanian National Institute of Metrology, Bucharest, Romania 555-560, 2001

[8] Mihai I., Marullo Reedtz G. “Optimisation of a potentiometric measurement system by calculation of the Allan variance,” in CPEM’02 Conf. Dig., pp, 48-49, 2002

[9] Allan D. W. “Should the classical variance be used as a basic measure in standards metrology?”, IEEE Trans. Instrum. Meas. IM-36, 646-654, 1987

[10] Witt T. J. Using the Allan variance and power spectral density to characterize DC nanovoltmeters. IEEE Trans. Instrum. Meas. 50, no. (2), pp. 445-448, 2001

[11] Mihai I. and Marullo Reedtz G. “Optimization of a potentiometric measurement system by calculation of the Allan variance.” Proceedings Conf. Prec. Electr. Meas. CPEM, Ottawa, Canada 48-49. 2002

[12] Galliana F, Capra P. P., Mihai I. “Measurement comparison between a commercial high resistance bridge and validated systems at ultra-high resistance values” IMEKO TC-4 2020 Palermo, Italy, September 14-16, 2020

APPENDIX. ANALYSIS OF THE DETECTOR AND THE NOISE.

Model 6514 is a 5½-digit high-performance system electrometer that can make current measurements at the minimum resolution of 0.1 fA on range of 20pA. The set of the two instruments, current detector, and its output circuit, can be represented as a unidirectional system characterized by a transfer function H_D and an input signal $x(t)$. The output signal $y(t)$ is a convolution system of $x(t)$ and H_D. The transfer function $H_D(f)$ is composed of the detector/electrometer transfer function and its analog output circuit. For the analysis of the power spectrum of the input signal $x(t)$, the current I_D , it is necessary to study the behavior of the $PSD_y(f)$ as a function of the frequency. For this scope it can be used an FFT analyzer.

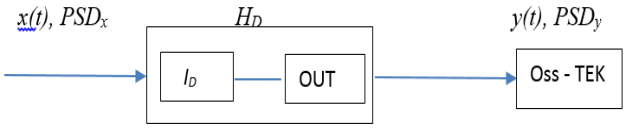

Figure 1. The current detector and the FFT analyzer (Oss –TEK) connected to its 2 V output.

The measurement unit for $PSD_y(f)$ is V^2/Hz. Usually a logarithmic representation is preferred for the both axes in order to observe the low frequency domain. In terms of the spectral power density, for the unidirectional system considered in Figure 1, it can be written:

$$PSD_x(f) = \frac{1}{|H_D(f)|^2} PSD_y(f) \tag{1}$$

Table 1. Example 2V analog output values.

Range	Applied signal	Analog output value (nominal)	Transfer function, H_D
20 pA	10.5 pA	-1.05 V	-100 mV/pA

For the noise evaluation from the equation (8), it used the free software program Stable32 to obtain the following values for the ratio 10T /MI :100T /GdL:

Table 2a. The Allan variation for 10T:100T(GdL) at 250 V

Tau, s	Min Sigma	Sigma	Max Sigma
1.00E-02	1.10E+00	1.11E+00	1.12E+00
2.00E-02	1.39E+00	1.41E+00	1.42E+00
4.00E-02	1.14E+00	1.16E+00	1.17E+00
8.00E-02	8.69E-01	8.88E-01	9.07E-01
1.60E-01	6.59E-01	6.79E-01	7.00E-01
3.20E-01	4.74E-01	4.94E-01	5.16E-01
6.40E-01	4.07E-01	4.31E-01	4.59E-01
1.28E+00	3.93E-01	4.25E-01	4.67E-01
2.56E+00	3.96E-01	4.41E-01	5.06E-01
5.12E+00	5.80E-01	6.73E-01	8.32E-01
1.02E+01	8.93E-01	1.09E+00	1.55E+00

Electrometers reads: **1.28 /0.02 = 64**

Table 2b. The Allan variation for 10T:100T(GdL) at 500 V

Tau, s	Min Sigma	Sigma	Max Sigma
1.00E-02	1.09E+00	1.10E+00	1.10E+00
2.00E-02	1.38E+00	1.40E+00	1.41E+00
4.00E-02	1.15E+00	1.17E+00	1.18E+00
8.00E-02	8.76E-01	8.94E-01	9.13E-01
1.60E-01	6.49E-01	6.68E-01	6.89E-01
3.20E-01	4.67E-01	4.86E-01	5.08E-01
6.40E-01	3.68E-01	3.90E-01	4.15E-01
1.28E+00	3.66E-01	3.96E-01	4.35E-01
2.56E+00	3.79E-01	4.22E-01	4.84E-01
5.12E+00	5.87E-01	6.80E-01	8.41E-01
1.02E+01	9.02E-01	1.11E+00	1.57E+00

Electrometers reads: **0.64 / 0.02 = 32**

Table 2c. The Allan variation for 10T:100T(GdL) at 750 V

Tau	Min Sigma	Sigma	Max Sigma
1.00E-02	1.09E+00	1.10E+00	1.10E+00
2.00E-02	1.38E+00	1.40E+00	1.41E+00
4.00E-02	1.13E+00	1.15E+00	1.16E+00
8.00E-02	8.72E-01	8.90E-01	9.10E-01
1.60E-01	6.55E-01	6.74E-01	6.95E-01
3.20E-01	4.83E-01	5.03E-01	5.26E-01
6.40E-01	3.91E-01	4.14E-01	4.41E-01
1.28E+00	4.05E-01	4.38E-01	4.81E-01
2.56E+00	4.09E-01	4.56E-01	5.23E-01
5.12E+00	5.93E-01	6.87E-01	8.49E-01
1.02E+01	8.99E-01	1.10E+00	1.56E+00

Electrometers reads: **0.64 / 0.02 = 32**

Table 2d. The Allan variation for 10T:100T(GdL) at 1000 V.

Tau	Min Sigma	Sigma	Max Sigma
1.00E-02	1.07E+00	1.08E+00	1.09E+00
2.00E-02	1.36E+00	1.38E+00	1.39E+00
4.00E-02	1.14E+00	1.16E+00	1.18E+00
8.00E-02	8.76E-01	8.94E-01	9.13E-01
1.60E-01	6.33E-01	6.52E-01	6.72E-01
3.20E-01	4.58E-01	4.77E-01	4.98E-01
6.40E-01	3.78E-01	4.00E-01	4.26E-01
1.28E+00	3.96E-01	4.28E-01	4.70E-01
2.56E+00	3.87E-01	4.31E-01	4.95E-01
5.12E+00	5.77E-01	6.69E-01	8.27E-01
1.02E+01	8.98E-01	1.10E+00	1.56E+00

Electrometers reads: **0.64 / 0.02 = 32**

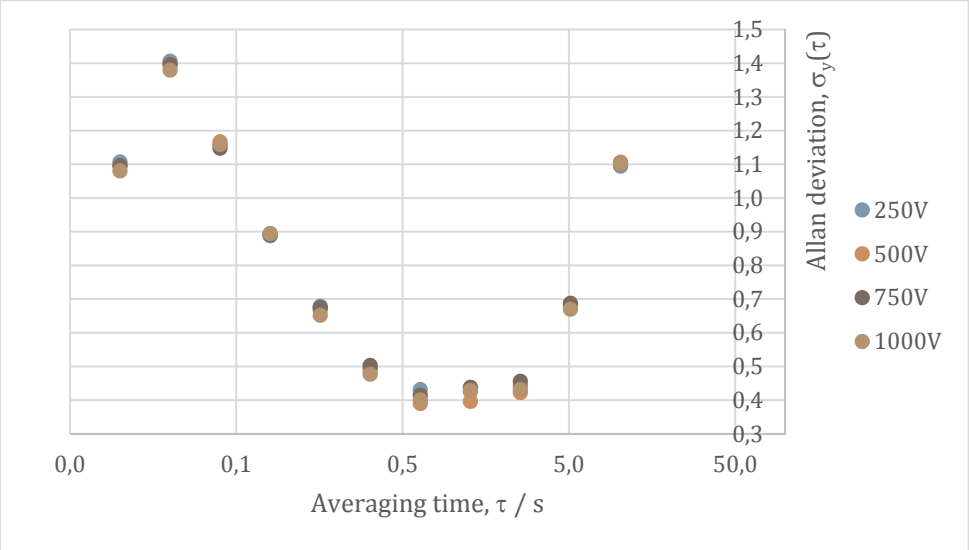

Using Table 6 from the paragraph *Evaluation of the intrinsic noise* of the dc sources, we can obtain for the white noise regime the relationship between the Allan deviation and the standard deviation. The result are reported in table 2.

$$\boldsymbol{\sigma_x}\,(\boldsymbol{N}) = \frac{1}{\sqrt{N}|H_D(f)|}\,\boldsymbol{\sigma_y}\,(\boldsymbol{\tau}) \tag{2}$$

Where N is number of the electrometer readings.

Table 2. Conversion from the minimum Allan variation (in white noise regime) to the standard deviation of the signal at the input of the detector.

Test, V	$\boldsymbol{\sigma_y(\tau)}$**,** mV	**Electrometer readings**	$\boldsymbol{\sigma_x}\,(\boldsymbol{N})$**,** fA
0	0.37	256	0.2
250	0.43	64	0.5
500	0.39	32	0.7
750	0.41	32	0.7
1000	0.40	32	0.7

Manual specification notes: Input bias current noise is < 0.75 fA p-p (0.1Hz to 10Hz bandwidth, damping on. Digital filter = 40 readings).

In Table 3 it is reported the calibration data for the Keithley 6514 sn: 4050338 in the range of 20 pA in the time period between 20 and 21 October 2021 using ULCA system and the calibration procedure PT-EM-3.2-06.

Table 3. 6514 calibration with procedure values PT-EM-3.2-06.

Nominal current	**Applied current, *I*a**	**Range**	**Gain,** Q = I_m / I_a	**Expanded uncertainty,** U(Q)
(pA)	(pA)	(pA)		(%)
+ 1.0	1.007518	20	1.0006011	0.160
- 1.0	-1.007715		1.0004046	0.160
+ 10.0	9.974542		1.0003114	0.017
- 10.0	-9.974563		1.0002941	0.017

Note: I_m is the current measured by the detector and I_a is the current applied by the calibration ULCA system.

CONTACT INFORMATION

Iulian Mihai was born in Focsani. Romania in 1972. He received the M.S. degrees in physics from the University of Physics from Bucharest in 1995 and in metrology engineering from the Polytechnic of Bucharest, Romania in 1998. In 1999 he joined the Istituto Elettrotecnico Nazionale "Galileo Ferraris (IEN) from Torino where he was involved in precision resistance measurements and quantum Hall effect during his Phd program studies. From 2005 to 2018 he was responsible of industrial accredited laboratories focusing on electrical and mechanical instruments calibration. From 2019 he joined the National Institute of Metrological Research (INRIM) Torino where he has been involved in precision high resistance measurements.

Istituto Nazionale di Ricerca Metrologica – INRIM
(www.inrim.it; www.inrim.eu)
Divisione Metrologia Applicata e Ingegneria
Strada delle Cacce 91
10135. Torino (Italy)
Tel. +39 011 3919337